Commun Nonlinear Sci Numer Simulat 31 (2016) 83–107

Contents lists available at ScienceDirect

Commun Nonlinear Sci Numer Simulat

journal homepage: www.elsevier.com/locate/cnsns

Periodic patterns and Pareto efficiency of state dependent impulsive controls regulating interactions between wild and transgenic mosquito populations

Hong Zhang [a], Paul Georgescu [b,*], Lai Zhang [c]

[a] Department of Financial Mathematics, Jiangsu University, Zhenjiang 212013, China
[b] Department of Mathematics, Technical University of Iaşi, Bd. Copou 11, Iaşi 700506, Romania
[c] Department of Mathematics and Mathematical Statistics, Umeå University, Umeå SE-90187, Sweden

ARTICLE INFO

Article history:
Received 1 November 2014
Revised 7 July 2015
Accepted 28 July 2015
Available online 4 August 2015

Keywords:
Transgenic mosquitoes
State-dependent impulsive perturbation
Order-1 periodic solution
orbital stability
Pareto efficiency
Pareto frontier

ABSTRACT

It is conceivable that genetically modified mosquitoes could stop the spread of malaria, by outcompeting the wild mosquitoes and interfering with their reproductive processes, and genetically inheriting and further transmitting a diminished potential to carry *Plasmodium*. To get insight into the possible outcomes, we formulate an ODE model for the interactions between wild and transgenic mosquito populations, which is subject to state-dependent impulsive perturbations. By first investigating the dynamics of the unperturbed system, we determine certain sufficient conditions for the existence and orbital stability of positive order-1 solution of the model system with state-dependent impulsive perturbations. Their feasibility is then illustrated by means of numerical simulations. In addition, to adequately control the wild mosquito population, we use a multi-target approach which, in addition to accounting for the total costs, keeps track of the total size of the wild mosquito population. To trade off these objectives, we consider the concept of Pareto efficiency to determine suitable control strategies which are near-optimal. Finally, we carry out numerical simulations to illustrate the Pareto frontier and then characterize the detailed Pareto efficient control regime.

1. Introduction

Anopheles maculipennis, the species of the genus *Anopheles* ("not of any benefit", from the Greek words *an*, "not" and *ophelos*, "benefit") was first described and classified by the German entomologist J. W. Meigen in 1818. Since R. Ross discovered in 1897 that *Anopheles* mosquitoes are able to transmit human malaria pathogen, *Plasmodium*, it has been observed that the transmission of malaria does not occur through human contact and that the mosquitoes in this genus are actually the sole malaria vectors [1]. Sickening over 200 million people and causing over 1 million deaths annually [2], malaria is, at the global scale, one of the most troublesome infectious diseases. Much efforts have been spent developing an effective vaccine over the past 30 years, as this would be an important step toward malaria prevention and control. However, this has been proved to be difficult, and only one candidate vaccine, RTS, S/AS01 has reached the stage of phase III clinical trials, with the prospect of being submitted for licensure in 2014 [3]. Unavailability of an effective vaccine has hampered so far the efforts to curtail the disease.

* Corresponding author. Tel.: +40 232 213737.
E-mail addresses: hongzhang@ujs.edu.cn (H. Zhang), v.p.georgescu@gmail.com (P. Georgescu), lai.zhang@umu.se (L. Zhang).

http://dx.doi.org/10.1016/j.cnsns.2015.07.013
1007-5704/

Alternatively, efforts have been focused on both targeting the evolution of *Plasmodium* in humans and on interrupting the transmission of the disease by the vector [1,4,5]. The most powerful and widely used approach to vector control is the use of insecticides. Four classes of insecticides are used for public health purposes (pyrethroids, organochlorines, organophosphates and carbamates), usually by means of long-lasting insecticide-treated nets and indoor residual spraying. While insecticides have been proved very successful in reducing disease incidence, resistance to insecticides among malaria vectors has emerged more than 25 years ago in America, Africa and Europe [6], frequently due to gene mutations that help the mosquitoes' nerve cells withstand insecticide attack, the acetylcholinesterase enzyme losing sensitivity to organophosphates and carbamates. Other forms of resistance, depending on increased levels of mosquito enzymes that can destroy pyrethroids before they reach their target, are also possible [7].

Since mosquitoes are the sole vectors for malaria transmission, rendering them incapable of transmitting malaria parasites could limit the spread of the disease. *In vivo* studies have led to the identification of a peptide, called SM1 peptide, that binds to the two epithelia which should be traversed by the parasite and inhibits their crossing [8]. By injecting mosquito embryos with a synthetic gene containing four SM1 units, four separate lines of transgenic mosquitoes have been obtained, the transgene being strongly induced in the midgut of the transgenic mosquitoes by a blood meal. The expression of SM1 peptide in the mosquitoes midgut drastically reduced their vector capability by inhibiting *Plasmodium* development. In two of three experiments, no transmission has been detected, while in a third one the transmission rate has been reduced to less than one third of its initial value. Also, the SM1 peptide did not alter mosquito fitness traits such as longevity and egg production.

Inheritable genetic transformations have been achieved for the genome of *Anopheles stephensi* mosquitoes by means of the *Minos* transposable element from *Drosophila hydei*, with the expectation that this technique can be successfully extended to the most prominent malaria vector, *Anopheles gambiae* [9,10]. Recently, the establishment of a stable *Wolbachia* infection in a population of *Anopheles stephensi* has also been reported [11]. The *Wolbachia* strain wAlbB derived from *Aedes albopictus* was observed to form a stable symbiosis with *Anopheles stephensi* and to have perfect maternal transmission together with high levels of cytoplasmic incompatibility (enhancing its capability to spread), while conferring resistance to *Plasmodium*, possibly by stimulating a mosquito antiparasitic immune response. Further, the wAlbB infection has been able to reach 100% infection frequency in a naturally uninfected population, under certain release conditions, and to remain fixed in subsequent generations. This establishes the feasibility of producing transgenic mosquitoes that have diminished potential to carry the parasite and provides a new and effective weapon against malaria.

Once pathogen refractory transgenic mosquitoes are obtained, the next step is to release them into the environment, with the goal of replacing the pathogen susceptible wild mosquitoes. However, transgenic mosquitoes can experience reduced fitness, due to various circumstances: inbreeding depression, random integration of transposable elements altering important genes or toxicity of a foreign protein expressed in abundance [12]. Also, it is suggested in [13,14] that the released mosquitoes would need to be nearly 100% refractory in order to have a real impact on malaria transmission. Such a high refractory capability would need multiple refractory genes, which may come with greater fitness impairment. In practice, it is almost impossible to replace the wild mosquito population with transgenic mosquitoes in any particular environment. In this regard, the strategic policies emphasize implementing effective and economical control mechanisms to keep the size of the wild mosquito population as low as reasonably practicable. Actually, the celebrated work [15] states as early as 1928 that "... in order to counteract malaria anywhere we need not banish *Anopheles* there entirely ... we need only to reduce their numbers below a certain figure".

A question arises about how transgenic mosquitoes should be released in combination with pesticide release in order to effectively control the abundance of wild mosquitoes. To address this question, which is the aim of this paper, we formulate a model for the interaction between wild and transgenic mosquito populations based on a two-dimensional ODE system with state-dependent impulsive perturbations. State-dependent impulsive dynamical systems are a particular case of hybrid systems in which the impulsive perturbations of a given continuous dynamical system occur whenever a threshold trigger is initiated [16,17]. In recent years, state-dependent impulsive control strategies have proved their usefulness in the study of dynamics of prey–predator systems [18,19], management of fisheries [20], integrated pest management [21], pulse vaccination for human infectious diseases [22], and chemostat models [23,24].

From a practical viewpoint, it is feasible to take a first step toward implementing state-dependent impulsive control strategies and estimate the sizes of adult and larval mosquito populations via landing rate counts and, respectively, a dipper and then take data back to the laboratory for an analysis of the catch. However, before releasing transgenic mosquitoes, other particulars of the target wild mosquito population such as its genetic diversity, mating behavior and heterogeneous biting should be analyzed, together with locations where the releases should occur. Also, one should have in mind that in malaria transmission the environmental ecology is complex in most locations [12], due to the complex life cycle of the parasite and to the fact that breeding sites are very transient due to uncontrollable external factors such as drying or flooding. Another question that needs further investigation is how transgenic mosquitoes should be released as a part of a state-dependent control strategy which involves also pesticide release.

Motivated by the above-mentioned considerations and by the ideas of [25,26], we formulate a model for the interaction between wild and transgenic mosquito populations based on a two-dimensional ODE system which is subject to state-dependent impulsive perturbations. Since determining genotype distributions for the offsprings in a variable environment is not simple, we group all transgenic populations into a single population, without distinguishing for their zygosity [25]. Also, we consider generation overlapping for both types of mosquitoes.

The paper is structured as follows. We first study our model system without perturbations (Section 3) and then derive sufficient conditions for the existence and orbital stability of positive order-1 solutions of our system with state-dependent impulsive

perturbations (Section 4). In Section 5, we use a multi-target approach to develop strategies for wild mosquito control which aim to keep the total cost as low as possible, while simultaneously remaining near optimal in the context of Pareto efficiency in terms of the total size of the wild mosquito population. We further numerically illustrate the Pareto frontier and the corresponding Pareto efficient controls. Our paper ends with several concluding remarks and a comparison between our results and those obtained in other works in the same field.

2. Model formulation

To derive our mathematical model, we rely upon the following assumptions regarding the interactions between wild and transgenic mosquitoes and the effects of insecticides.

- A.1 All transgenic mosquitoes are considered as a single population group, without regard for their zygosity.
- A.2 Transgenic and wild mosquito populations share the same habitat and have the same saturation-density-dependent death rate.
- A.3 In the absence of one mosquito population, the growth of the other is given by a logistic law.
- A.4 Larval and adult mosquito populations may be easily monitored by using dippers and, respectively, mechanical traps. However, it is difficult for inspectors to distinguish between wild and transgenic mosquitoes on site. Hence, the control mechanism is triggered when the total density of wild and transgenic mosquitoes reaches a threshold value H^*.
- A.5 All mosquitoes with a transgenic mosquito ancestor are unable to transmit malaria.
- A.6 Once pesticides are released, the densities of wild and transgenic individuals experience a sharp decrease.

Based on above assumptions and inspired by the ideas in [25,26], our mathematical model, which accounts for the interactions between wild and transgenic mosquitoes and for the effects of the insecticide coupled with the release of transgenic mosquitoes, can be stated in the following form

$$\begin{cases} \left.\begin{aligned} \frac{\mathrm{d}M(t)}{\mathrm{d}t} &= \frac{a_1M(t)+b_1T(t)}{M(t)+T(t)}M(t)\left(1-\frac{M(t)+T(t)}{K}\right)-\delta M(t) \doteq f_1(M,T),\\ \frac{\mathrm{d}T(t)}{\mathrm{d}t} &= \frac{a_2M(t)+b_2T(t)}{M(t)+T(t)}T(t)\left(1-\frac{M(t)+T(t)}{K}\right)-\delta T(t) \doteq f_2(M,T), \end{aligned}\right\} T+M<H^*,\\ \left.\begin{aligned} M(t^+) &= (1-m_1)M(t),\\ T(t^+) &= (1-m_2)T(t)+U, \end{aligned}\right\} T+M=H^*. \end{cases} \tag{1}$$

Here, $M(t)$ and $T(t)$ are the densities of the wild mosquito and transgenic mosquito populations at time t, respectively. The constants a_1 and b_1 denote the recruitment rates of wild mosquitoes through mating with wild and transgenic mosquitoes, respectively. The constants a_2 and b_2 denote the recruitment rates of transgenic mosquitoes through mating with wild and transgenic mosquitoes, respectively. We denote by K the total carrying capacity of the environment with respect to both mosquito classes, while δ denotes the saturation-density dependent death rate, the same for both mosquito classes.

When the total density of wild and transgenic mosquitoes reaches the threshold value H^*, control measures are taken, in the form of spraying insecticides and releasing transgenic mosquitoes. As a result of spraying insecticides, fixed proportions of the wild and transgenic populations, denoted by m_1 and m_2, respectively, are removed instantaneously. We denote by U the constant amount of transgenic mosquitoes released each time the control measures are implemented.

Remark 2.1. From a biological viewpoint, it makes sense to assume that $H^* < K$, that is, the threshold value which, when reached, triggers the usage of impulsive control mechanisms is lower than the total carrying capacity of the environment. Since the time instances at which the impulsive control measures are taken are not prescribed *a priori*, but depend instead on the total density of the mosquito populations, our control model can be classified as being one with state-dependent perturbations. The concrete values of m_1, m_2 and U generally depend upon environmental factors [27].

3. Dynamics of the unperturbed system

To better understand the dynamics of the system (1), we start by investigating the corresponding Kolmogorov-type unperturbed system of ordinary differential equations consisting of the first two equations in (1)

$$\begin{cases} \frac{\mathrm{d}M(t)}{\mathrm{d}t} = \frac{a_1M(t)+b_1T(t)}{M(t)+T(t)}M(t)\left(1-\frac{M(t)+T(t)}{K}\right)-\delta M(t),\\ \frac{\mathrm{d}T(t)}{\mathrm{d}t} = \frac{a_2M(t)+b_2T(t)}{M(t)+T(t)}T(t)\left(1-\frac{M(t)+T(t)}{K}\right)-\delta T(t), \end{cases} \tag{2}$$

which characterizes the dynamics of (1) between two "beats", that is, between two consecutive impulsive perturbations. The first step toward establishing the well-posedness and relevance of (2) is to obtain a feasible domain, together with sufficient conditions for the existence and stability of equilibria of system (2).

3.1. The feasible domain

The standard positivity argument for Kolmogorov systems (see, for instance, [28], Section 2 or [29], Lemma 1) shows that a solution $(M(t), T(t))$ of (2) which starts at $t = t_0$ with strictly positive component-wise data $(M(t_0), T(t_0))$ remains strictly positive component-wise for all $t \geq t_0$. In addition, one remarks that $\frac{dM}{dt}|_{M+T=K} < 0$ and $\frac{dT}{dt}|_{M+T=K} < 0$ and consequently the bounded triangle

$$\Omega = \{(x, y) | x > 0,\ y > 0 \text{ and } 0 < x + y < K\}$$

is a feasible domain for the system (2).

3.2. Existence of equilibria

It is easy to see that the semi-trivial equilibria of (2) are given by

$$E_1 = \left(0, \frac{K}{b_2}(b_2 - \delta)\right), \quad E_2 = \left(\frac{K}{a_1}(a_1 - \delta), 0\right),$$

which exist and are nontrivial if and only if $b_2 > \delta$ and $a_1 > \delta$, respectively. Therefore, both semi-trivial equilibria E_1 and E_2 exist if and only if

$$\min\{a_1, b_2\} > \delta, \tag{3}$$

which means that the recruitment rates through mating with the same mosquito class should be greater than the saturation-density dependent death rate for both mosquito populations.

We now find conditions for the existence of a positive equilibrium $E^* = (M^*, T^*)$. It is seen from (2) that necessarily

$$(a_1 - a_2)M^* = (b_2 - b_1)T^*,$$

which leads to

$$M^* = \frac{K(b_2 - b_1)}{a_1(b_2 - b_1) + b_1(a_1 - a_2)}(\delta^* - \delta), \quad T^* = \frac{K(a_1 - a_2)}{a_1(b_2 - b_1) + b_1(a_1 - a_2)}(\delta^* - \delta), \tag{4}$$

with

$$\delta^* = \frac{a_1(b_2 - b_1) + b_1(a_1 - a_2)}{(b_2 - b_1) + (a_1 - a_2)}.$$

Hence, there exists a unique positive equilibrium if and only if

$$(a_1 - a_2)(b_2 - b_1) > 0 \text{ and } \delta^* > \delta, \tag{5}$$

which means that no mosquito class should be able to outcompete the other through having larger respective recruitment rates, since $a_1 - a_2$ and $b_1 - b_2$ have opposite signs, and that both classes are able to avoid extinction since the "averaged" reproduction rate δ^* is larger than the death rate δ.

We summarize the results of the existence, nonexistence and coexistence of the equilibria of the system (2) in Table 1.

3.3. Local stability of equilibria

We now investigate the stability of the semi-trivial equilibria of the system (2). Linearizing the system (2) near the equilibria $E_1 = \left(0, \frac{K}{b_2}(b_2 - \delta)\right)$ and $E_2 = \left(\frac{K}{a_1}(a_1 - \delta), 0\right)$, respectively, yields the Jacobian matrices

$$J(E_1) = \begin{bmatrix} \left(\frac{b_1}{b_2} - 1\right)\delta & 0 \\ * & -(b_2 - \delta) \end{bmatrix}$$

and

$$J(E_2) = \begin{bmatrix} -(a_1 - \delta) & * \\ 0 & \left(\frac{a_2}{a_1} - 1\right)\delta \end{bmatrix},$$

in which $*$ represents elements of the Jacobian matrices $J(E_1)$ and $J(E_2)$, respectively, which are not involved in the computation of the corresponding eigenvalues and consequently do not need to be specified. Then, under the assumption (3), it is seen that E_1 is locally asymptotically stable if $b_1 < b_2$ and E_2 is locally asymptotically stable if $a_2 < a_1$, while if the converse inequalities hold, then the respective equilibria are unstable. We thus have the following theorem.

Theorem 3.1.

(i) *The semi-trivial equilibrium E_1 exists and is locally asymptotically stable (node) if*

$$b_2 > \max\{b_1, \delta\}. \tag{6}$$

Table 1
Summary table of the existence, nonexistence and coexistence of the equilibria with the corresponding necessary and sufficient conditions.

Case	Existing equilibrium	Nonexisting equilibrium	Necessary and sufficient conditions
1	E_1, E_2, E^*		$\delta < \min\{a_1, b_2, \delta^*\}, (a_1-a_2)(b_2-b_1) > 0$
2	E_1, E_2	E^*	$\delta^* < \delta < \min\{a_1, b_2\}, (a_1-a_2)(b_2-b_1) > 0$ or $\delta < \min\{a_1, b_2\}, (a_1-a_2)(b_2-b_1) < 0$
3	E_1, E^*	E_2	$a_1 < \delta < \min\{b_2, \delta^*\}, (a_1-a_2)(b_2-b_1) > 0$
4	E_2, E^*	E_1	$b_2 < \delta < \min\{a_1, \delta^*\}, (a_1-a_2)(b_2-b_1) > 0$
5	E_1	E_2, E^*	$\max\{\delta^*, a_1\} < \delta < b_2, (a_1-a_2)(b_2-b_1) > 0$ or $a_1 < \delta < b_2, (a_1-a_2)(b_2-b_1) < 0$
6	E_2	E_1, E^*	$\max\{\delta^*, b_2\} < \delta < a_1, (a_1-a_2)(b_2-b_1) > 0$ or $b_2 < \delta < a_1, (a_1-a_2)(b_2-b_1) < 0$
7	E^*	E_1, E_2	$\max\{a_1, b_2\} < \delta < \delta^*, (a_1-a_2)(b_2-b_1) > 0$

(ii) *The semi-trivial equilibrium E_1 exists but is unstable (saddle point) if*

$$b_1 > b_2 > \delta. \tag{7}$$

(iii) *The semi-trivial equilibrium E_2 exists and is locally asymptotically stable (node) if*

$$a_1 > \max\{a_2, \delta\}. \tag{8}$$

(iv) *The semi-trivial equilibrium E_2 exists but is unstable (saddle point) if*

$$a_2 > a_1 > \delta. \tag{9}$$

Remark 3.2. Condition $b_2 > b_1$ indicates that the transgenic mosquitoes reproduce better with the same class, producing on average more offsprings per mating through mating with transgenic mosquitoes than with mating with wild mosquitoes. Condition $a_1 > a_2$ has a similar interpretation with regard to the reproductive abilities of wild mosquitoes.

Remark 3.3. From the analysis of the existence and stability conditions (6)–(9), one deduces that the existence and stability of E_1 are independent of the existence and stability of E_2, and *vice versa*.

To investigate the stability of the unique positive equilibrium $E^* = (M^*, T^*)$, we assume that the existence condition (5) holds. Linearizing the system (2) around the equilibrium E^* yields the Jacobian matrix

$$J(E^*) = \begin{bmatrix} M^*\left(\frac{T^*(a_1-b_1)}{(M^*+T^*)^2} - \frac{a_1}{K}\right) & M^*\left(\frac{M^*(b_1-a_1)}{(M^*+T^*)^2} - \frac{b_1}{K}\right) \\ T^*\left(\frac{T^*(a_2-b_2)}{(M^*+T^*)^2} - \frac{a_2}{K}\right) & T^*\left(\frac{M^*(b_2-a_2)}{(M^*+T^*)^2} - \frac{b_2}{K}\right) \end{bmatrix}.$$

We first note that, by (4), the following identities hold

$$a_1M^* + b_1T^* = K(\delta^* - \delta), \quad M^* + T^* = \left(1 - \frac{\delta}{\delta^*}\right)K = \frac{\delta^* - \delta}{\delta^*}K.$$

To apply Routh–Hurwitz stability conditions, we first see that

$$\begin{aligned} \operatorname{tr} J(E^*) &= \frac{M^*T^*(a_1 - a_2 + b_2 - b_1)}{(M^* + T^*)^2} - \frac{a_1M^* + b_2T^*}{K} \\ &= \frac{(b_2 - b_1)(a_1 - a_2)}{b_2 - b_1 + a_1 - a_2} - (\delta^* - \delta), \end{aligned} \tag{10}$$

and

$$\begin{aligned} \det J(E^*) &= M^*T^*\left(\frac{1}{M^* + T^*}\frac{1}{K}(a_2b_1 - a_1b_2) + \frac{1}{K^2}(a_1b_2 - a_2b_1)\right) \\ &= \frac{M^*T^*}{K}(a_2b_1 - a_1b_2)\left(\frac{1}{M^* + T^*} - \frac{1}{K}\right) \\ &= -\frac{M^*T^*}{K}(a_1(b_2 - b_1) + b_1(a_1 - a_2))\frac{1}{K}\frac{\delta}{\delta^* - \delta} \\ &= -\frac{(b_2 - b_1)(a_1 - a_2)}{a_1(b_2 - b_1) + b_1(a_1 - a_2)}(\delta^* - \delta)\delta. \end{aligned} \tag{11}$$

Using (10) and (11), one obtains that

$$(\operatorname{tr} J(E^*))^2 - 4\det J(E^*) \tag{12}$$

$$= \left(\frac{(b_2-b_1)(a_1-a_2)}{b_2-b_1+a_1-a_2} - (\delta^*-\delta)\right)^2 + 4\frac{(b_2-b_1)(a_1-a_2)}{a_1(b_2-b_1)+b_1(a_1-a_2)}(\delta^*-\delta)\delta. \tag{13}$$

This implies

$$\begin{aligned}(\operatorname{tr} J(E^*))^2 - 4\det J(E^*) &= \left(\frac{(b_2-b_1)(a_1-a_2)}{b_2-b_1+a_1-a_2} + (\delta^*-\delta)\right)^2 - 4\frac{(b_2-b_1)(a_1-a_2)}{b_2-b_1+a_1-a_2}(\delta^*-\delta)\\ &\quad + 4\frac{(b_2-b_1)(a_1-a_2)}{a_1(b_2-b_1)+b_1(a_1-a_2)}(\delta^*-\delta)\delta\\ &= \left(\frac{(b_2-b_1)(a_1-a_2)}{b_2-b_1+a_1-a_2} + (\delta^*-\delta)\right)^2\\ &\quad + 4\frac{(b_2-b_1)(a_1-a_2)}{a_1(b_2-b_1)+b_1(a_1-a_2)}(\delta^*-\delta)\left(-\frac{a_1(b_2-b_1)+b_1(a_1-a_2)}{b_2-b_1+a_1-a_2}+\delta\right)\\ &= \left(\frac{(b_2-b_1)(a_1-a_2)}{b_2-b_1+a_1-a_2} + (\delta^*-\delta)\right)^2 - 4\frac{(b_2-b_1)(a_1-a_2)}{a_1(b_2-b_1)+b_1(a_1-a_2)}(\delta^*-\delta)^2.\end{aligned} \tag{14}$$

Assuming that the existence condition (5) holds, which implies in particular that b_2-b_1 and a_1-a_2 have the same sign, one obtains from Routh–Hurwitz conditions and (11) that if E^* is stable, then necessarily $b_1 > b_2$ and $a_2 > a_1$. In this situation, one sees using also (10) and (14) that

$$\operatorname{tr} J(E^*) < 0, \quad \det J(E^*) > 0, \quad (\operatorname{tr} J(E^*))^2 - 4\det J(E^*) > 0.$$

Note also that if $b_1 < b_2$ and $a_1 > a_2$, then

$$\det J(E^*) < 0, \quad (\operatorname{tr} J(E^*))^2 - 4\det J(E^*) > 0.$$

Then the following existence and stability results for the unique positive equilibrium hold.

Theorem 3.4.

(i) *Suppose that*

$$b_1 > b_2, \quad a_2 > a_1, \quad \delta^* > \delta.$$

Then there exists a unique positive equilibrium E^*, which is a stable node.

(ii) *Suppose that*

$$b_1 < b_2, \quad a_2 < a_1, \quad \delta^* > \delta.$$

Then there exists a unique positive equilibrium E^*, which is a saddle point.

Remark 3.5. The inequalities in Theorem 3.4 can be interpreted in a manner similar to the considerations given in Remark 3.2.

Remark 3.6. Suppose that all three equilibria E_1, E_2 and E^* exist. It then follows from Theorems 3.1 and 3.4 that if E^* is stable on Ω, then E_1 and E_2 are both unstable, and *vice versa*.

From the above discussion and the Routh–Hurwitz conditions, one then obtains the following result.

Corollary 3.1. *Suppose that the condition (5) holds. Then there exists a unique positive equilibrium E^*, which is a saddle point if $b_1 < b_2$ or $a_2 < a_1$.*

3.4. The nonexistence of periodic solutions

Suppose that

$$a_1 + b_2 < b_1 + a_2,$$

that is, on average, mosquitoes reproduce better with members of the other species rather than with members of their own. Let us denote by $\mathcal{F}_{\mathcal{M}}$ and $\mathcal{F}_{\mathcal{T}}$ the right-hand sides of the equations composing (2). Then there exists a function

$$\nu : \Omega \to \mathbb{R}, \quad \nu(M,T) = M^{-1}T^{-1},$$

such that

$$\frac{\partial}{\partial M}(\nu\mathcal{F}_{\mathcal{M}})+\frac{\partial}{\partial T}(\nu\mathcal{F}_{\mathcal{T}})=\frac{a_1-b_1}{(M+T)^2}-\frac{a_1}{KT}+\frac{b_2-a_2}{(M+T)^2}-\frac{b_2}{KM}$$
$$=\frac{(a_1+b_2)-(b_1+a_2)}{(M+T)^2}-\frac{a_1}{KT}-\frac{b_2}{KM}<0.$$

According to the Bendixson–Dulac criterion, the system (2) has no periodic solution remaining entirely within Ω.

4. Dynamics of the system with state-dependent impulses

In this section, we shall investigate the occurrence of periodic behavior as $t\to\infty$, under a suitable strategy relying on the administration of pesticides and the release of transgenic mosquitoes. This is of importance from a practical viewpoint, since understanding behavioral patterns well enough may help devising an optimal control scenario.

We start by introducing certain notations, preliminary definitions and auxiliary results, referring also the reader to the appendices whenever needed. Let us define the "control line" Γ_{H^*} on which the control measures are prompted by

$$\Gamma_{H^*}\doteq\left\{(M,T)|M>0,\ T>0 \text{ and } M+T=H^*\right\}.$$

For any point $P_n\in\Gamma_{H^*}$, suppose that the trajectory $O^+(P_n,t_n)$ starting from the initial point P_n intersects the control line Γ_{H^*} infinitely many times. We then define the Poincaré map of the section Γ_{H^*} by

$$M_{n+1}=\mathcal{F}(M_n,m_1,m_2,U,H^*)\ (\text{or } T_{n+1}=\mathcal{G}(T_n,m_1,m_2,U,H^*)). \tag{15}$$

Definition 4.1. A trajectory $O^+(P_n,t_n)$ of the system (1) is said to be order-k periodic if there exists a positive integer $k\geq 1$ such that k is the smallest integer for $M_{n+k}=M_n$ (or $T_{n+k}=T_n$).

It is then seen that the initial value problem for the system (1) is biologically well-posed, in the sense that the trajectories of (1) are positivity-preserving.

Lemma 4.1. *Assume that $(M(t),T(t))$ is a solution of the system (1) with the initial condition $(M(t_0),T(t_0))\in\Omega$. Then $\left(M(t),T(t)\right)\in\mathbf{R}^2_+$ for all $t\geq t_0$.*

Proof. For any initial value $(M(t_0),T(t_0))\in\Omega$, we shall discuss the following two possibilities given by the number of possible contacts between the solution $(M(t),T(t))$ and the line Γ_{H^*}.

(a) In the first case, let us consider that the solution $(M(t),T(t))$ reaches Γ_{H^*} infinitely many times, at time instances t_k, $k=1,2,\cdots,t_k\to\infty$ as $k\to\infty$. If the conclusion of Lemma 4.1 is false, we then obtain that there exists a positive integer n and a $t^*\in(t_{n-1},t_n]$ such that $\min\{M(t^*),T(t^*)\}=0$ and $M(t)>0,T(t)>0$ for $t_0\leq t<t^*$. The first possibility is that $M(t^*)=0$, $T(t^*)>0$. In this regard, it follows from the first and third equations of the system (1) that

$$M(t^*)>(1-m_1)^{n-1}M(t_0)\exp\left(-\int_{t_0}^{t^*}\max\{a_1,b_1\}\left(\frac{T(s)+M(s)}{K}+\delta\right)ds\right)>0,$$

which contradicts the fact that $M(t^*)=0$. The second possibility is that $T(t^*)=0$. In this regard, it follows from the second and fourth equations of the system (1) that

$$T(t^*)>(1-m_2)^{n-1}T(t_0)\exp\left(-\int_{t_0}^{t^*}\max\{a_2,b_2\}\left(\frac{T(s)+M(s)}{K}+\delta\right)ds\right)$$
$$+U\sum_{t_0<t_k<t^*}\exp\left(-\int_{t_k}^{t^*}\max\{a_2,b_2\}\left(\frac{T(s)+M(s)}{K}+\delta\right)ds\right)>0,$$

which contradicts the fact that $T(t^*)=0$.

(b) The second case, in which the solution $(M(t),T(t))$ reaches Γ_{H^*} finitely many times, can be treated in a similar way.

Hence, according to the above discussion, one finds that $M(t)>0$ and $T(t)>0$ for all $t\geq t_0$. This completes the proof. □

4.1. Existence of positive order-1 periodic solution

In this subsection, we shall give some sufficient conditions for the existence of positive periodic solutions under certain additional assumptions.

First of all, let us assume that both the wild and transgenic mosquitoes have the same insecticide-related death rate, that is

$$m_1\equiv m_2.$$

Let us also observe that after the control measures are employed the total size of the mosquito population becomes

$$H^{**}\doteq(1-m_1)H^*+U=(1-m_2)H^*+U.$$

We then define the following "retreat line" $\Gamma_{H^{**}}$, to which the solutions of the system (1) jump immediately after the control measures are taken, by

$$\Gamma_{H^{**}} \doteq \left\{(M,T)|M>0,\ T>0 \text{ and } M+T=H^{**}\right\}.$$

In order for the control measures to be effective, it is required that $H^{**}<H^{*}$, which means the total size of the mosquito population decreases after control measures are employed. This inequality is equivalent to

$$U < m_1H^* = m_2H^*.$$

For the sake of convenience, let us denote the nullclines for the wild and transgenic mosquitoes, respectively, by

$$\mathcal{M}_1 \doteq \left\{(M,T)|M\geq 0,\ T\geq 0 \text{ and } M\left(\frac{a_1M+b_1T}{M+T}(1-\frac{M+T}{K})-\delta\right)=0\right\}$$

and

$$\mathcal{T}_1 \doteq \left\{(M,T)|M\geq 0,\ T\geq 0 \text{ and } T\left(\frac{a_2M+b_2T}{M+T}(1-\frac{M+T}{K})-\delta\right)=0\right\}.$$

Since we cannot compute explicitly the analytic expressions of the positive order-1 periodic solutions due to the nonlinear structure of the unperturbed system (note at this point that one does not know any relationship between a_1, a_2, b_1, b_2 beforehand) and to the additional layer of complexity represented by the state-dependent nature of the control, we have to resort to a geometric approach. This approach essentially consists in locating the iterations of the Poincaré map of the retreat line $\Gamma_{H^{**}}$ via an analysis of the direction field of the unperturbed system. To perform such an analysis and to establish the geometric properties of the trajectories, one needs to know first and foremost the relative position of the equilibria and of the nullclines with respect to the control line Γ_{H^*} and the retreat line $\Gamma_{H^{**}}$. Having the trapezium determined by the control line, the retreat line and the semi-axes completely on one side of a nullcline eases the geometric analysis, while having the trapezium on both sides makes it more difficult. Also, stable equilibria should be positioned behind the control line in order to make sure that control measures really occur.

To investigate the existence of positive order-1 periodic solutions, we shall consider in what follows three broad situations which correspond to all cases in Table 1. In fact, this classification scheme depends only upon the dynamic behavior of the system (2) because the trajectories of the system (1) between two successive impulses are characterized by the dynamics of the ODE system (2).

(𝕀) The system (2) does not have a positive equilibrium

We first consider the situation in which the system (2) does not have a positive equilibrium, which corresponds to **Case** 2, **Case** 5 and **Case** 6 in Table 1. Also, one or both of the equilibria E_1 and E_2 are assumed to be stable.

We claim that the system (1) has no order-1 periodic solution only if E_1 is stable and $K(b_1-\delta)\leq b_1H^{**}$.

Suppose that the system (1) admits only the equilibrium E_1 (**Case** 5 in Table 1), and assume also that E_1 is stable and $K(b_1-\delta)\leq b_1H^{**}$. Suppose further that $H^*<\frac{K}{b_2}(b_2-\delta)$, which indicates that the impulsive control mechanisms are eventually triggered by all solutions trying to reach E_1.

Let $P_1(\varepsilon_{1p}, H^{**}-\varepsilon_{1p})\in\Gamma_{H^{**}}$ for any $\varepsilon_{1p}\in(0,H^{**})$. According to the geometrical structure of the phase field of the system (1), the trajectory $O^+(P_1,t_0)$ starting from the point P_1 will approach E_1 and then intersect the section Γ_{H^*} at the point $F_1(S_1,H^*-S_1)$. At the point F_1, the trajectory $O^+(P_1,t_0)$ jumps to the point $P_2((1-m_1)S_1, H^{**}-(1-m_1)S_1)$ due to the effects of the impulsive perturbations $M(t^+)=(1-m_1)M(t)$ and $T(t^+)=(1-m_1)T(t)+U$, which occurs when $M(t)+T(t)=H^*$.

Obviously, the condition that $K(b_1-\delta)\leq b_1H^{**}$ includes the following two cases. The first one is $b_1<\delta$, which, together with condition $a_1<\delta$ given in **Case** 5 of Table 1, implies that

$$\frac{dM}{dt}|_{P_1} < \varepsilon_{1p}\left(\delta\left(1-\frac{H^{**}}{K}\right)-\delta\right)<0.$$

The other is $b_1>\delta$, which, together with conditions $K(b_1-\delta)\leq b_1H^{**}$ and $a_1<\delta$, also implies that

$$\begin{aligned}\frac{dM}{dt}|_{P_1} &= \varepsilon_{1p}\left(\frac{-(b_1-a_1)\varepsilon_{1p}+b_1H^{**}}{H^{**}}\left(1-\frac{H^{**}}{K}\right)-\delta\right)\\ &= \varepsilon_{1p}\frac{-(b_1-a_1)\varepsilon_{1p}(K-H^{**})-(b_1H^{**}-(b_1-\delta)K)H^{**}}{KH^{**}}\\ &< 0.\end{aligned}$$

It is then seen from the above that $\frac{dM}{dt}|_{P_1}<0$ in both cases. In addition, one notes that E_1 is a unique equilibrium and is a stable node. It then follows from the structure of the direction field and of the phase portrait (see Fig. 1) together with Lemma 4.1 that $S_1<\varepsilon_{1p}$, which indicates that $(1-m_1)S_1<\varepsilon_{1p}$. Hence, the system (1) has no order-1 periodic solution.

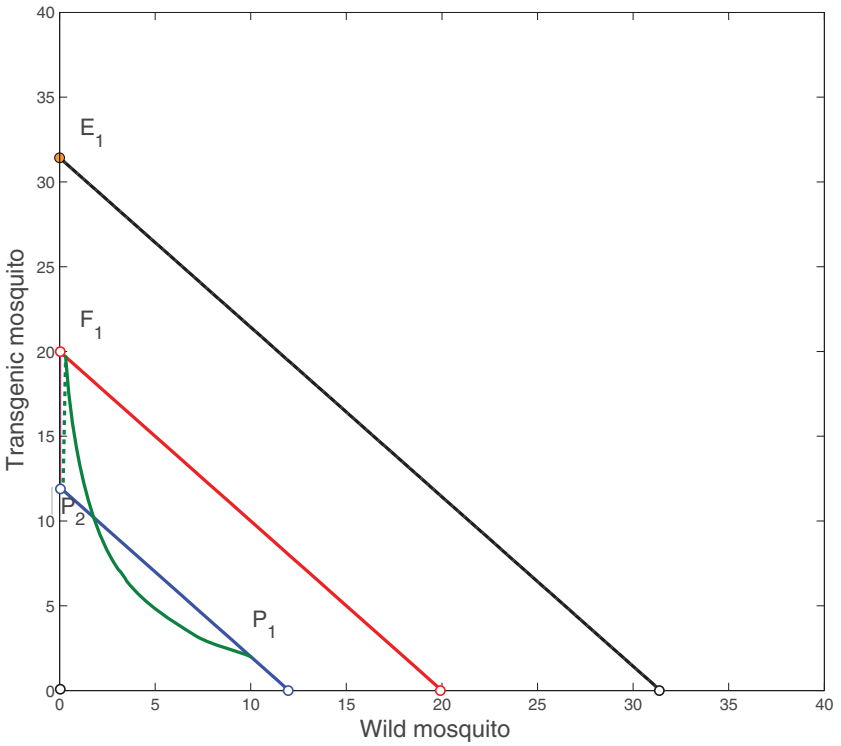

Fig. 1. Dynamical behavior of the system (1). Here, $H^* = 20$, $H^{**} = 12$, $m_1 = m_2 = 0.5$, $a_1 = 0.2$, $a_2 = 0.7$, $b_1 = 0.2$, $b_2 = 0.7$, $\delta = 0.48$, $K = 100$ and $U = 2$. The red line represents the set Γ_{H^*}, the blue line represents the set $\Gamma_{H^{**}}$, the black curve represents the nullcline for transgenic mosquitoes in the first quadrant and the green curve represents the trajectory $O^+(P_1, t_0)$ starting from the point P_1 and then intersecting the section Γ_{H^*} at the point F_1. At the point F_1, the trajectory $O^+(P_1, t_0)$ jumps to the point P_2. (For interpretation of the references to colour in this figure legend, the reader is referred to the web version of this article.)

Next, we claim that there exists a positive order-1 periodic solution of the system (1) if E_1 is stable and $K(b_1 - \delta) > b_1 H^{**}$. In fact, since $b_1 > a_1$ and $K > H^{**}$, we can find $P_1(\varepsilon_{1p}, H^{**} - \varepsilon_{1p}) \in \Gamma_{H^{**}}$ together with

$$\varepsilon_{1p} < \frac{H^{**}(K(b_1 - \delta) - b_1 H^{**})}{(K - H^{**})(b_1 - a_1)},$$

which implies that $\frac{dM}{dt}|_{P_1} > 0$. It is easy to choose a $\Delta t > 0$ and an m_1 such that $M(t_0 + \Delta t) > \varepsilon_{1p}$ and then $(1 - m_1)M(t_0 + \Delta t) = \varepsilon_{1p}$. Additionally, choose a $U \in (0, H^{**})$ such that $H^* = \frac{H^{**} - U}{1 - m_1} > H^{**}$. Hence, for a given retreat line $\Gamma_{H^{**}}$, we can determine the control line such that the point $\big(M(t + \Delta t), T(t + \Delta t)\big)$ coincides with the point F_1, which indicates that $(1 - m_1)S_1 = \varepsilon_{1p}$. On the other hand, given a control line, we can then determine the corresponding retreat line such that $(1 - m_1)S_1 = \varepsilon_{1p}$, which implies that the system (1) has a positive order-1 periodic solution.

Suppose now that there is only one stable equilibrium $E_2 = (\frac{K}{a_1}(a_1 - \delta), 0)$. Let us also assume that $H^* < \frac{K}{a_1}(a_1 - \delta)$, for a reason similar to the one outlined above.

Also, let $P_1(\varepsilon_{1p}, H^{**} - \varepsilon_{1p}) \in \Gamma_{H^{**}}$ for any $\varepsilon_{1p} \in (0, H^{**})$. According to the geometrical structure of the phase field of the system (1), the trajectory $O^+(P_1, t_0)$ starting from the point P_1 will approach E_2 and then intersect the section Γ_{H^*} at the point $F_1(S_1, H^* - S_1)$. At the point F_1, the trajectory $O^+(P_1, t_0)$ will jump to the point $P_2((1 - m_1)S_1, H^{**} - (1 - m_1)S_1)$, due to the same impulsive control mechanisms.

Obviously, since E_2 is a unique equilibrium and a stable node, it follows from the structure of the direction field and of the phase portrait (see Fig. 2) that if $H^{**} - (1 - m_1)S_1 < H^{**} - \varepsilon_{1p}$ or $H^{**} - (1 - m_1)S_1 > H^{**} - \varepsilon_{1p}$, then the system (1) has no order-1 periodic solution. Otherwise, if $(1 - m_1)S_1 = \varepsilon_{1p}$, then the system (1) admits a positive order-1 periodic solution (see Fig. 3).

Finally, if assume that there are bistable semi-trivial equilibria, according to the discussion above, we then conclude that the system (1) also admits at least one order-1 periodic solution near the stable equilibrium E_2 if $H^{**} - (1 - m_1)S_1 = H^{**} - \varepsilon_{1p}$ as shown in Fig. 4.

(Ⅲ) System (2) has a unique unstable positive equilibrium

We now assume that there is a unique unstable positive equilibrium of the system (2), which corresponds to certain parts of **Case** 1, **Case** 3 and **Case** 4 in Table 1. It follows from the above-mentioned analysis and Table 1 that if there exists a stable

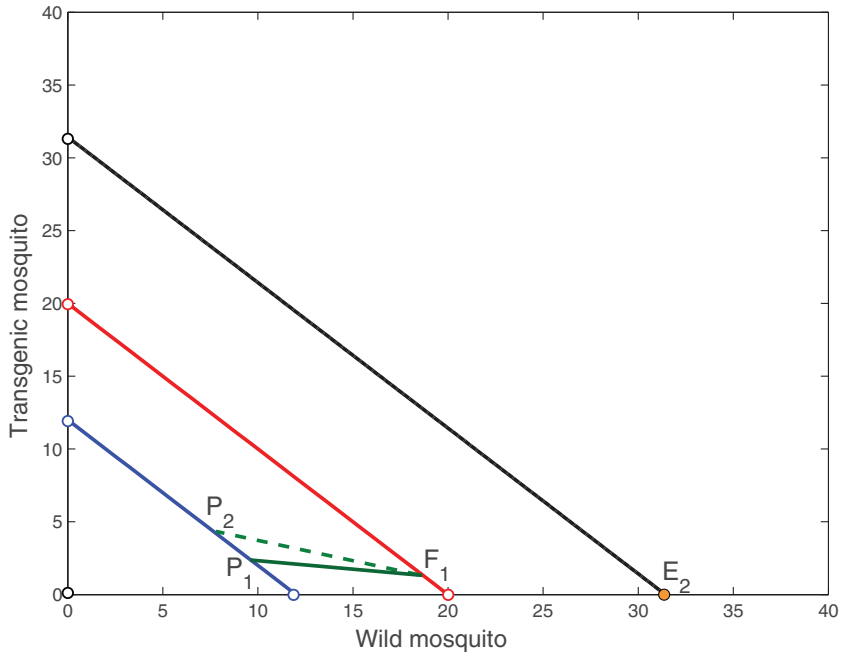

Fig. 2. Dynamical behavior of the system (1). Here, $H^* = 20$, $H^{**} = 12$, $a_1 = 0.7$, $a_2 = 0.2$, $b_1 = 0.7$, $b_2 = 0.5$, $\delta = 0.48$ and $K = 100$. The red line represents the set Γ_{H^*}, the blue line represents the set $\Gamma_{H^{**}}$, the black curve represents the nullcline for wild mosquitoes in the first quadrant and the green curve represents the trajectory $O^+(P_1, t_0)$ starting from the point P_1 and then intersecting the section Γ_{H^*} at the point F_1. At the point F_1, the trajectory $O^+(P_1, t_0)$ jumps to the point P_2. It is easily to find suitable m_1, m_2 and U such that $H^{**} - (1 - m_1)S_1 < H^{**} - \varepsilon_{1p}$ (or $H^{**} - (1 - m_1)S_1 > H^{**} - \varepsilon_{1p}$), which implies the point P_2 is on the right of P_1 (or on the left of P_1). (For interpretation of the references to colour in this figure legend, the reader is referred to the web version of this article.)

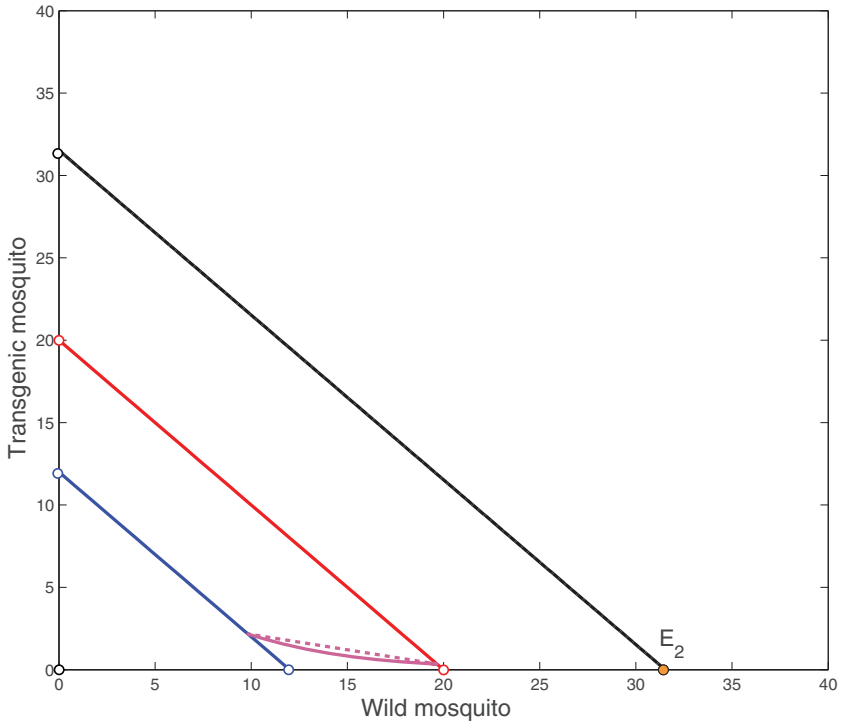

Fig. 3. The system (1) has a (purple) positive order-1 periodic solution. Here, $H^* = 20$, $H^{**} = 12$, $m_1 = m_2 = 0.5$, $a_1 = 0.7$, $a_2 = 0.2$, $b_1 = 0.7$, $b_2 = 0.5$, $\delta = 0.48$, $K = 100$ and $U = 2$. The red line represents the set Γ_{H^*}, the blue line represents the set $\Gamma_{H^{**}}$, the black curve represents the nullcline for wild mosquitoes in the first quadrant and the purple curve represents a positive order-1 periodic solution. (For interpretation of the references to colour in this figure legend, the reader is referred to the web version of this article.)

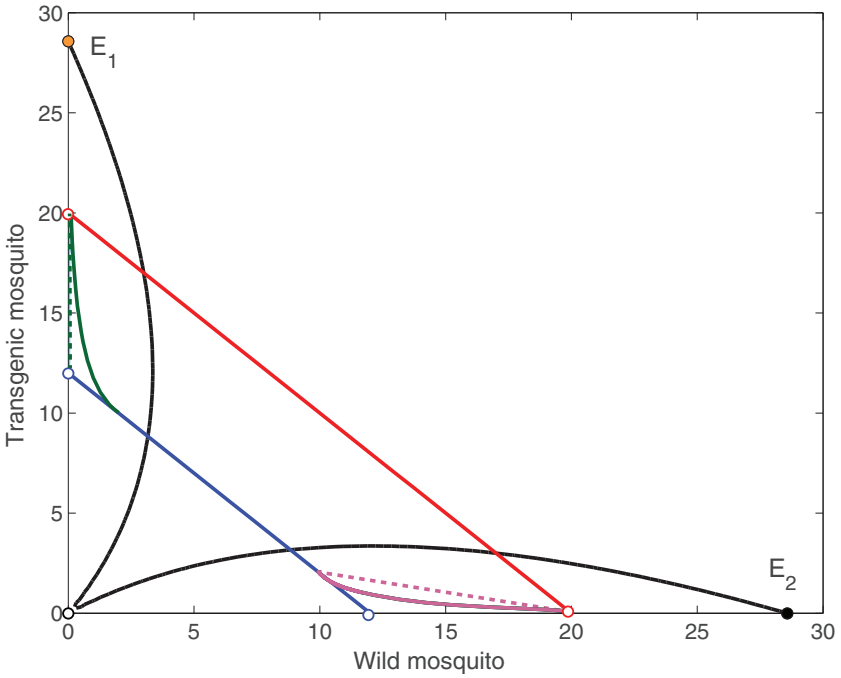

Fig. 4. The system (1) has a (purple) positive order-1 periodic solution near the stable equilibrium E_2. Here, $H^* = 20$, $H^{**} = 12$, $m_1 = m_2 = 0.5$, $a_1 = 0.7$, $a_2 = 0.2$, $b_1 = 0.2$, $b_2 = 0.7$, $\delta = 0.5$, $K = 100$ and $U = 2$. The red line represents the set Γ_{H^*}, the blue line represents the set $\Gamma_{H^{**}}$, the black curves represent the nullclines for wild and transgenic mosquitoes in the first quadrant and the purple curve represents a positive order-1 periodic solution. (For interpretation of the references to colour in this figure legend, the reader is referred to the web version of this article.)

semi-trivial equilibrium E_1 and $K(b_1 - \delta) > b_1 H^{**}$, or if there exists the stable equilibrium E_2, then the system (1) admits at least one positive order-1 periodic solution as shown in Figs. 5 and 6.

(𝕀𝕀𝕀) System (2) has a unique stable positive equilibrium

We now assume that the system (2) has a unique positive equilibrium (M^*, T^*), which is an asymptotically stable node. In addition, it is also assumed that $M^* + T^* > H^*$, which means that the impulsive control mechanisms are eventually triggered. In the following, we consider four possibilities for the existence of the positive periodic solutions in the first quadrant.

(i) Assume that the intersection of $\Gamma_{H^{**}}$ and $\mathcal{M}_1$ is the empty set and the intersection of $\Gamma_{H^{**}}$ and $\mathcal{T}_1$ is also the empty set. Let us denote the domains

$$I \doteq \{(M, T) | M' > 0 \text{ and } T' > 0\}$$

and

$$I_{H^*} \doteq \{(M, T) | M > 0, T > 0 \text{ and } M + T \leq H^*\}.$$

Let $P_1(\varepsilon_{1p}, H^{**} - \varepsilon_{1p}) \in \Gamma_{H^{**}}$, for an arbitrarily small positive ε_{1p}. According to the geometrical structure of the phase field of the system (1), the trajectory $O^+(P_1, t_0)$ starting from the point P_1 will remain within the domain $I \doteq \{(M, T) | M' > 0 \text{ and } T' > 0\}$ and then intersect the line Γ_{H^*} at the point $F_1(S_1, H^* - S_1)$. At the point F_1, the trajectory $O^+(P_1, t_0)$ jumps to the point $P_2((1 - m_1)S_1, H^{**} - (1 - m_1)S_1)$ due to the effects of the impulsive perturbations $M(t^+) = (1 - m_1)M(t)$ and $T(t^+) = (1 - m_2)T(t) + U$, when $M(t) + T(t) = H^*$, and subsequently reaches the point $F_2(S_2, H^* - S_2)$. If there exists an m^* such that $(1 - m^*)S_1 = \varepsilon_{1p}$, then P_1 coincides with P_2, which indicates that F_1 also coincides with F_2. Otherwise, Lemma 4.1 and the choice of a small positive ε_{1p} guarantees that, for any $U > 0$, there exists an m^* such that $(1 - m^*)S_1 > \varepsilon_{1p}$ and then $(1 - m^*)(H^* - S_1) + U < H^{**} - \varepsilon_{1p}$ since the reason that $I_{H^*} \subset I$ implies that $S_1 > \varepsilon_{1p}$ and $H^* - S_1 > H^{**} - \varepsilon_{1p}$, which indicates that P_1 is on the left of P_2. One then notes that F_2 is on the right of F_1. Otherwise, the trajectory P_1F_1 and the trajectory P_2F_2 can intersect at some point, which contradicts the uniqueness of solutions for the system (2) without impulsive effects. Therefore, it follows from (15) that $S_2 = \mathcal{F}(S_1, m_1, m_2, U, H^*)$ and

$$\mathcal{F}(S_1, m_1, m_2, U, H^*) - S_1 = S_2 - S_1 > 0. \tag{16}$$

On the other hand, let $A_1(H^{**} - \varepsilon_{1p}, \varepsilon_{1p}) \in \Gamma_{H^{**}}$ for arbitrarily small positive ε_{1p}. Then the trajectory $O^+(A_1, t_0)$ starting from the point A_1 will remain within the domain I and then intersect the segment Γ_{H^*} at the point $B_1(S_1, H^* - S_1)$. At

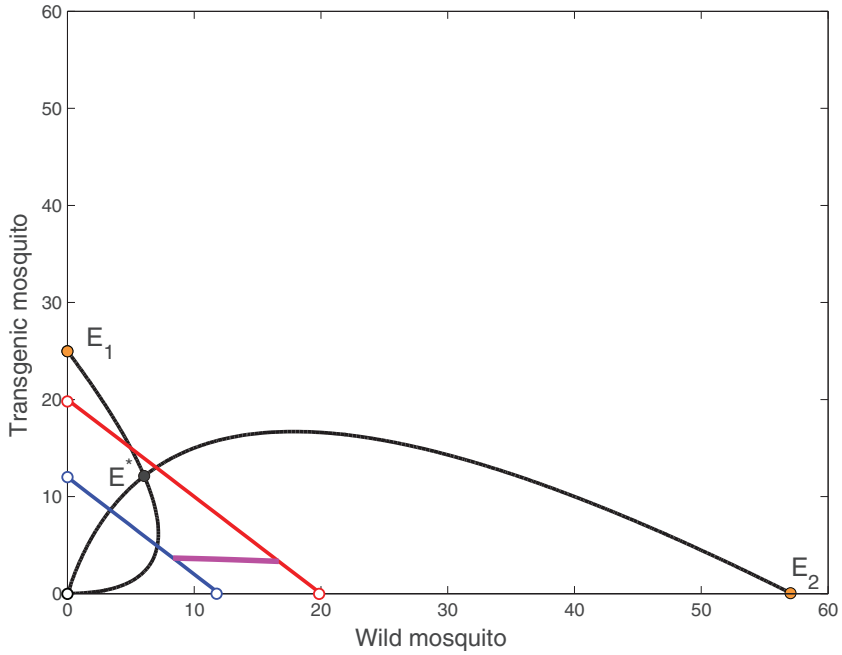

Fig. 5. The system (1) has a (purple) positive order-1 periodic solution. Here, $H^* = 20$, $H^{**} = 12$, $m_1 = m_2 = 0.5$, $a_1 = 0.7$, $a_2 = 0.3$, $b_1 = 0.2$, $b_2 = 0.4$, $\delta = 0.3$, $K = 100$ and $U = 2$. The red line represents the set Γ_{H^*}, the blue line represents the set $\Gamma_{H^{**}}$, the black curves represent the nullclines for wild and transgenic mosquitoes in the first quadrant and the purple curve represents a positive order-1 periodic solution. (For interpretation of the references to colour in this figure legend, the reader is referred to the web version of this article.)

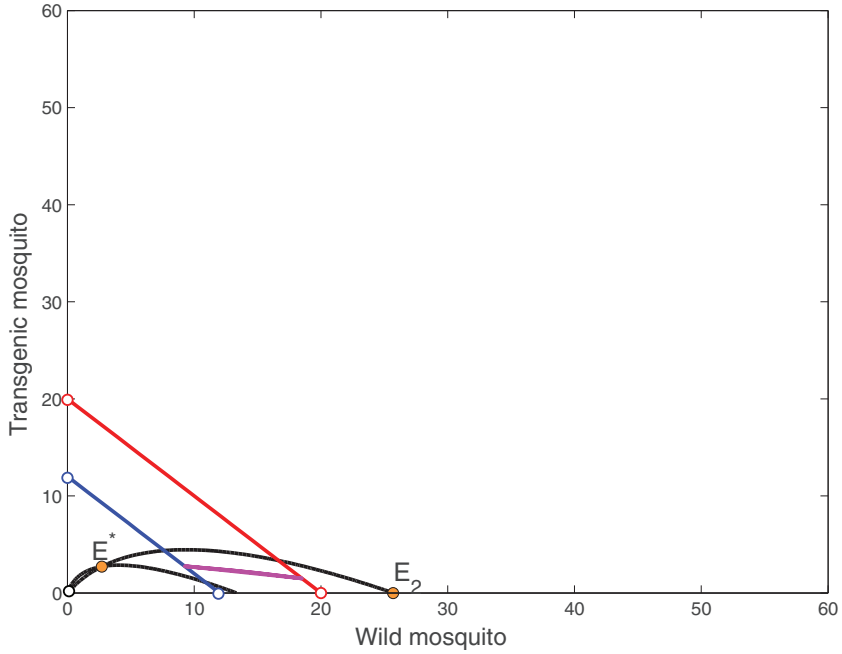

Fig. 6. The system (1) has a (purple) positive order-1 periodic solution. Here, $H^* = 20$, $H^{**} = 12$, $m_1 = m_2 = 0.5$, $a_1 = 0.7$, $a_2 = 0.6$, $b_1 = 0.4$, $b_2 = 0.5$, $\delta = 0.52$, $K = 100$ and $U = 2$. The red line represents the set Γ_{H^*}, the blue line represents the set $\Gamma_{H^{**}}$, the black curves represent the nullclines for wild and transgenic mosquitoes in the first quadrant and the purple curve represents a positive order-1 periodic solution. (For interpretation of the references to colour in this figure legend, the reader is referred to the web version of this article.)

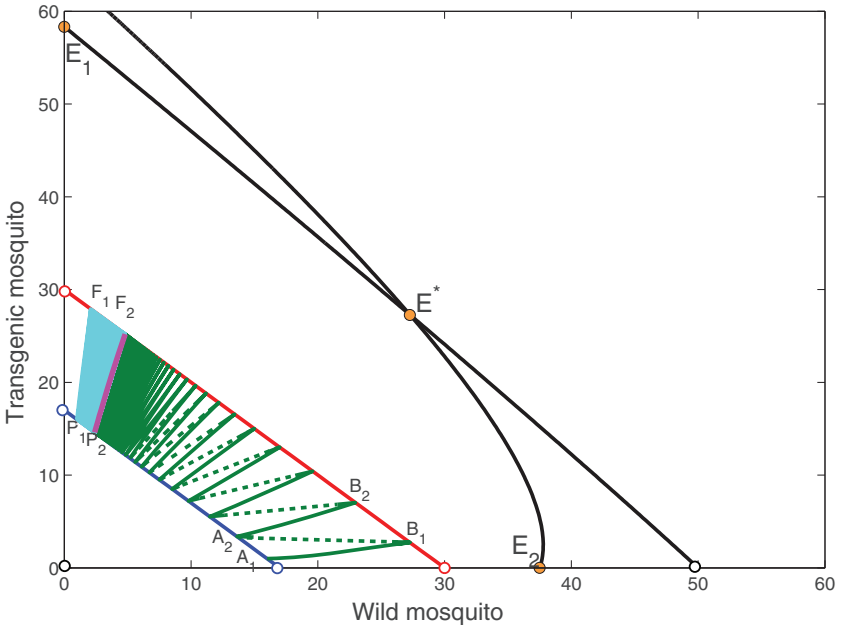

Fig. 7. The system (1) has a (purple) positive order-1 periodic solution. Here, $H^* = 30$, $H^{**} = 17$, $m_1 = m_2 = 0.5$, $a_1 = 0.4$, $a_2 = 0.5$, $b_1 = 0.7$, $b_2 = 0.6$, $\delta = 0.25$, $K = 100$ and $U = 2$. The red line represents the set Γ_{H^*}, the blue line represents the set $\Gamma_{H^{**}}$, the black curves represent the nullclines for wild and transgenic mosquitoes in the first quadrant and the purple curve represents a positive order-1 periodic solution. (For interpretation of the references to colour in this figure legend, the reader is referred to the web version of this article.)

the point B_1, the trajectory $O^+(A_1, t_0)$ jumps to the point $A_2((1-m_1)S_1, H^{**} - (1-m_1)S_1)$ due to the effects of impulsive control mechanisms and then intersects the segment Γ_{H^*} again at the point $B_2(S_2, H^* - S_2)$.

If there exists an m^{**} such that $(1-m^{**})S_1 = H^{**} - \varepsilon_{1p}$, then A_1 coincides with A_2, which indicates that B_1 coincides with B_2. Otherwise, since $I_{H^*} \subset I$, Lemma 4.1 and arbitrarily small positive ε_{1p} guarantees that, for the above-mentioned m^*, there exists a $U > 0$ such that $(1-m^*)(H^* - S_1) + U > \varepsilon_{1p}$ implies that $H^{**} - \varepsilon_{1p} > (1-m^*)S_1$, which indicates that A_1 is on the right of A_2. Subsequently, one notes that B_2 is on the left of B_1. Otherwise, the trajectory A_1B_1 and the trajectory A_2B_2 can intersect at some point, which contradicts the uniqueness of solutions for the system (2) without impulsive effects.

Therefore, it follows from (15) that $S_2 = \mathcal{F}(S_1, m_1, m_2, U, H^*)$ and

$$\mathcal{F}(S_1, m_1, m_2, U, H^*) - S_1 = S_2 - S_1 < 0. \tag{17}$$

To sum it up, it follows from the above discussion that when $S_1 = S_2$, the system (1) has a positive order-1 periodic solution. Also, by (16) and (17), the Poincaré map (15) has a fixed point [30], which means the system (1) also has a positive order-1 periodic solution as shown in Fig. 7.

(ii) Assume that the intersection of $\Gamma_{H^{**}}$ and the curve $\mathcal{M}_1$ is not the empty set, while, however, the intersection of $\Gamma_{H^{**}}$ and the curve $\mathcal{T}_1$ is the empty set.

Let $P_1(\varepsilon_{1p}, H^{**} - \varepsilon_{1p}) \in \Gamma_{H^{**}}$ for arbitrarily small ε_{1p}. According to the geometrical structure and the phase field of the system (1), the trajectory $O^+(P_1, t_0)$ starting from the point P_1 remains within the domain $I \doteq \{(M, T) | M' > 0 \text{ and } T' > 0\}$ and then intersects the segment Γ_{H^*} at the point $F_1(S_1, H^* - S_1)$. At the point F_1, the trajectory $O^+(P_1, t_0)$ jumps to the point $P_2((1-m_1)S_1, H^{**} - (1-m_1)S_1)$ due to the effects of the impulsive perturbations $M(t^+) = (1-m_1)M(t)$ and $T(t^+) = (1-m_2)T(t) + U$, which occur when $M(t) + T(t) = H^*$ and subsequently reaches the point $F_2(S_2, H^* - S_2)$.

If there exists an m^* such that $(1-m^*)S_1 = \varepsilon_{1p}$, then P_1 coincides with P_2, which indicates that F_1 also coincides with F_2. Otherwise, for any $U > 0$, there exists an m^* such that $(1-m^*)S_1 > \varepsilon_{1p}$ and $(1-m^*)(H^* - S_1) + U < H^{**} - \varepsilon_{1p}$ because $S_1 > \varepsilon_{1p}$ and then $H^* - S_1 > H^{**} - \varepsilon_{1p}$, which indicates that P_1 is on the left of P_2. Also, one then notes that F_2 is on the right of F_1. Therefore, it follows from (15) that $S_2 = \mathcal{F}(S_1, m_1, m_2, U, H^*)$ and

$$\mathcal{F}(S_1, m_1, m_2, U, H^*) - S_1 = S_2 - S_1 > 0. \tag{18}$$

On the other hand, one notes that the point of intersection between $\Gamma_{H^{**}}$ and $\mathcal{M}_1$ is $P_M^* = \left(M^{**}, H^{**} - M^{**}\right)$, where $M^{**} = \frac{KH^{**}(\delta - b_1) + b_1 H^{**2}}{(K - H^{**})(a_1 - b_1)}$.

Let us consider two cases, in which one is that $A_1(M^{**} - \varepsilon_{1p}, H^{**} - M^{**} + \varepsilon_{1p}) \in \Gamma_{H^{**}}$ for arbitrarily small positive ε_{1p} (see Fig. 8) and the other is that $A_1(M^{**} + \varepsilon_{1p}, H^{**} - M^{**} - \varepsilon_{1p}) \in \Gamma_{H^{**}}$ for arbitrarily small positive ε_{1p} (see Fig. 9).

First, if A_1 belongs to the domain I, then the trajectory $O^+(A_1, t_0)$ starting from the point A_1 remains within the domain I and then intersects the segment Γ_{H^*} at the point $B_1(S_1, H^* - S_1)$. After reaching the point B_1, the trajectory $O^+(A_1, t_0)$

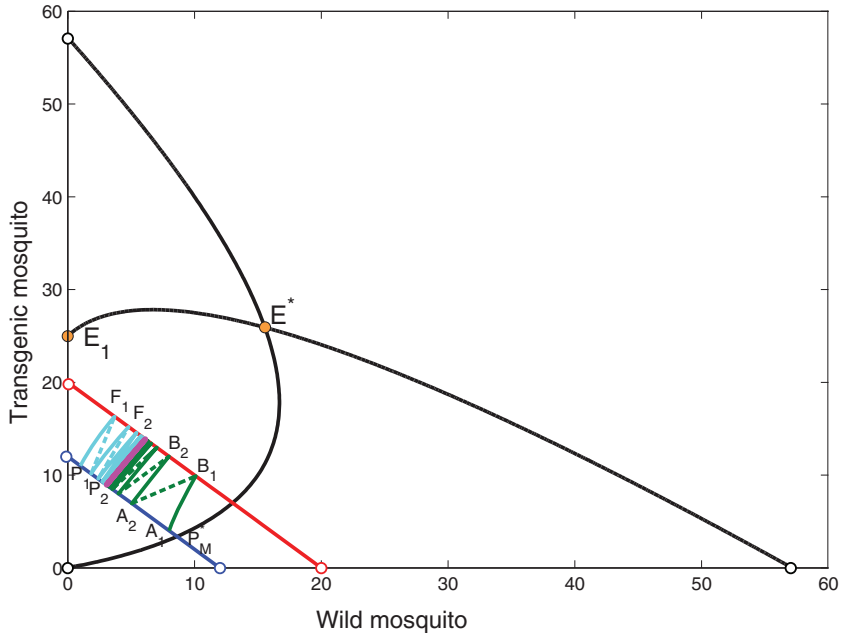

Fig. 8. The system (1) has a (purple) positive order-1 periodic solution. Here, $H^* = 20$, $H^{**} = 12$, $m_1 = m_2 = 0.5$, $a_1 = 0.1$, $a_2 = 0.5$, $b_1 = 0.7$, $b_2 = 0.5$, $\delta = 0.2$, $K = 100$ and $U = 2$. The red line represents the set Γ_{H^*}, the blue line represents the set $\Gamma_{H^{**}}$, the black curves represent the nullclines for wild and transgenic mosquitoes in the first quadrant and the purple curve represents a positive order-1 periodic solution. (For interpretation of the references to colour in this figure legend, the reader is referred to the web version of this article.)

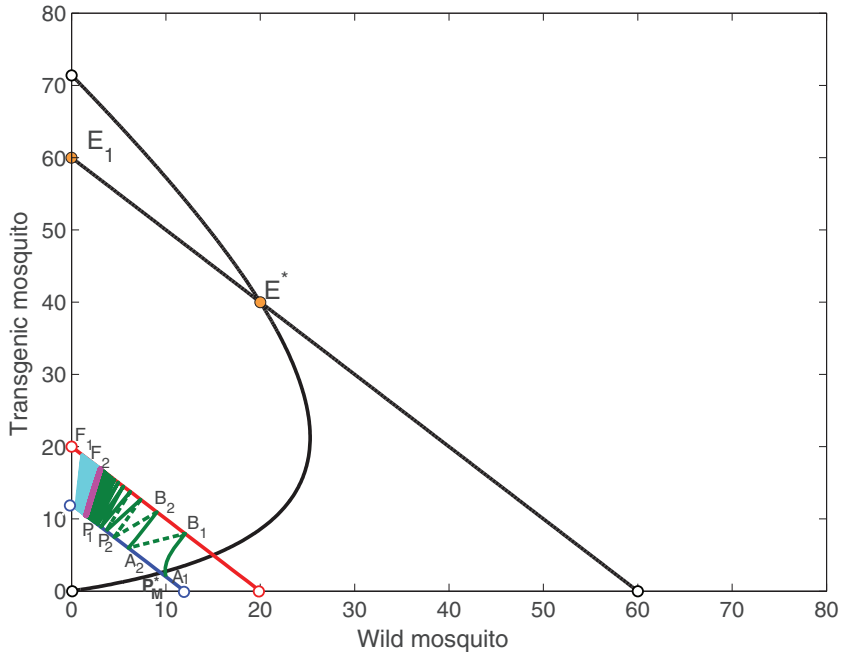

Fig. 9. The system (1) has a (purple) positive order-1 periodic solution. Here, $H^* = 20$, $H^{**} = 12$, $m_1 = m_2 = 0.5$, $a_1 = 0.1$, $a_2 = 0.5$, $b_1 = 0.7$, $b_2 = 0.5$, $\delta = 0.2$, $K = 100$ and $U = 2$. The red line represents the set Γ_{H^*}, the blue line represents the set $\Gamma_{H^{**}}$, the black curves represent the nullclines for wild and transgenic mosquitoes in the first quadrant and the purple curve represents a positive order-1 periodic solution. (For interpretation of the references to colour in this figure legend, the reader is referred to the web version of this article.)

jumps to the point $A_2((1-m_1)S_1, H^{**}-(1-m_1)S_1)$ due to the effects of the impulsive control measures and then intersects the segment Γ_{H^*} again at the point $B_2(S_2, H^*-S_2)$.

If there exists an m^{**} such that $(1-m^{**})S_1 = H^{**}-\varepsilon_{1p}$, then A_1 coincides with A_2, which indicates that B_1 coincides with B_2. If A_1 and A_2 do not coincide, we claim that, for the above-mentioned m^*, there exists a $U>0$ such that A_1 is on the right of A_2. In fact, for the above-mentioned m^*, there exists a $U>0$ such that $(1-m^*)(H^*-S_1)+U > H^{**}-M^{**}+\varepsilon_{1p}$ and then $(1-m^*)S_1 < M^{**}-\varepsilon_{1p}$ imply that the trajectory $O^+(A_1,t_0)$ jumps to the point A_2, which is on the left of A_1, then A_2 should remain in the domain I.

Second, if A_1 belongs to the domain $II \doteq \{(M,T)|M'<0 \text{ and } T'>0\}$, then according to the phase field of the system (2) the trajectory $O^+(A_1,t_0)$ moves across the boundary of the domain II and enters the domain I, which implies that the trajectory $O^+(A_1,t_0)$ should intersect the segment Γ_{H^*} at $B_1 \in I$. After reaching the point B_1, the trajectory $O^+(A_1,t_0)$ jumps to the point A_2 due to the effects of the impulsive control measures and then intersects the segment Γ_{H^*} again at the point $B_2(S_2, H^*-S_2)$. Similarly, we claim that for the above-mentioned m^* there exists a $U>0$ such that A_1 is on the right of A_2. One then notes that

$$\mathcal{F}(S_1,m_1,m_2,U,H^*)-S_1 = S_2-S_1 < 0. \tag{19}$$

To sum it up, it follows from the above discussion that when $S_1=S_2$, the system (1) has a positive order-1 periodic solution. Also, by (18) and (19), the Poincaré map (15) has a fixed point, which means the system (1) has a positive order-1 periodic solution, as shown in Figs. 8 and 9.

(iii) Assume that the intersection of $\Gamma_{H^{**}}$ and the curve $\mathcal{M}_1$ is an empty set, while, however, the intersection of $\Gamma_{H^{**}}$ and the curve $\mathcal{T}_1$ is not an empty set.

Let $A_1(H^{**}-\varepsilon_{1p},\varepsilon_{1p}) \in \Gamma_{H^{**}}$ for arbitrarily small positive ε_{1p}. According to the geometrical structure and the phase field of the system (1), the trajectory $O^+(P_1,t_0)$ starting from the point A_1 will remain within the domain I and then intersect the segment Γ_{H^*} at the point $B_1(S_1, H^*-S_1)$. At the point B_1, the trajectory $O^+(A_1,t_0)$ jumps to the point $A_2((1-m_1)S_1, H^{**}-(1-m_1)S_1)$ due to the effects of the impulsive control measures and subsequently reaches the point $B_2(S_2, H^*-S_2)$. It is obvious that $S_1 > H^{**}-\varepsilon_{1p}$ and $H^*-S_1>\varepsilon_{1p}$. So if there exists an m^{**} such that $(1-m^{**})S_1 = H^{**}-\varepsilon_{1p}$, then A_1 coincides with A_2, which indicates that B_1 also coincides with B_2. Otherwise, for any $m^* \in (0,1)$, there exists a $U>0$ such that $(1-m^*)(H^*-S_1)+U>\varepsilon_{1p}$ implies that $H^{**}-\varepsilon_{1p} > (1-m^*)S_1$, which indicates that A_1 is on the right of A_2. One notes that B_2 is on the left of B_1. Otherwise, the trajectory A_1B_1 and the trajectory A_2B_2 can intersect at some point, which contradicts the uniqueness of solutions for the system (2). Therefore, it follows from (15) that $S_2 = \mathcal{F}(S_1,m_1,m_2,U,H^*)$ and

$$\mathcal{F}(S_1,m_1,m_2,U,H^*)-S_1 = S_2-S_1 < 0. \tag{20}$$

On the other hand, one notes that the intersection point between $\Gamma_{H^{**}}$ and $\mathcal{T}_1$ is $T_M^* = \left(H^{**}-T^{**}, T^{**}\right)$, where $T^{**} = \frac{KH^{**}(\delta-a_2)+a_2H^{**2}}{(K-H^{**})(b_2-a_2)}$. In what follows we consider two cases, in which one is that $P_1(H^{**}-T^{**}+\varepsilon_{1p}, T^{**}-\varepsilon_{1p}) \in \Gamma_{H^{**}}$ for arbitrarily small positive ε_{1p} (see Fig. 10) and the other is $P_1(H^{**}-T^{**}-\varepsilon_{1p}, T^{**}+\varepsilon_{1p}) \in \Gamma_{H^{**}}$ for arbitrarily small positive ε_{1p} (see Fig. 11).

First, if P_1 belongs to the domain I, then the trajectory $O^+(P_1,t_0)$ starting from the point P_1 will remain within the domain I and then intersect the segment Γ_{H^*} at the point $F_1(S_1, H^*-S_1)$. At the point F_1, the trajectory $O^+(P_1,t_0)$ jumps to the point $P_2((1-m_1)S_1, H^{**}-(1-m_1)S_1)$ due to the effects of the impulsive control mechanisms and then intersects the section Γ_{H^*} again at the point $F_2(S_2, H^*-S_2)$. It is obvious that $S_1 > H^{**}-T^{**}+\varepsilon_{1p}$ and $H^*-S_1 > T^{**}-\varepsilon_{1p}$. If there exists an m^{**} such that $(1-m^{**})S_1 = H^{**}-T^{**}+\varepsilon_{1p}$, then P_1 coincides with P_2, which indicates that F_1 coincides with F_2. Otherwise, if P_1 does not coincide with P_2, we claim that, for the above-mentioned U, there exists an $m^* \in (0,1)$ such that P_1 is on the left of P_2. In fact, for the above-mentioned U, there exists an $m^* \in (0,1)$ such that $(1-m^*)(H^*-S_1)+U < T^{**}-\varepsilon_{1p}$ and then $H^{**}-T^{**}+\varepsilon_{1p} < (1-m^*)S_1$, which indicate that the point P_2 is on the right of P_1. Therefore, it follows from (15) that $S_2 = \mathcal{F}(S_1,m_1,m_2,U,H^*)$ and

$$\mathcal{F}(S_1,m_1,m_2,U,H^*)-S_1 = S_2-S_1 > 0. \tag{21}$$

Second, if P_1 belongs to the domain $III \doteq \{(M,T)|M'>0 \text{ and } T'<0\}$, we may then obtain the same result by applying the similar analysis. To sum it up, it follows from the above discussion that when $S_1=S_2$, the system (1) has a positive order-1 periodic solution. Also, by (20) and (21), the Poincaré map (15) has a fixed point, which means that the system (1) has a positive order-1 periodic solution, as shown in Figs. 10 and 11.

(iv) Assume that the intersection of $\Gamma_{H^{**}}$ and the curve $\mathcal{M}_1$ is not the empty set and, similarly, the intersection of $\Gamma_{H^{**}}$ and the curve $\mathcal{T}_1$ is not the empty set. We hereby consider four cases: $A_1 \in I$, $P_1 \in I$; $A_1 \in I$, $P_1 \in III$; $A_1 \in II$, $P_1 \in I$; $A_1 \in II$, $P_1 \in III$. According to the arguments employed for Cases *i–iii*, it is seen that the system (1) has a positive order-1 periodic solution, as shown in Figs. 12 and 13.

Subsequently, assume that insecticide toxicity to wild mosquitoes is different from the insecticide toxicity to transgenic mosquitoes. Without loss of generality, we assume that $m_1 > m_2$, which means insecticide toxicity to wild mosquitoes is stronger than insecticide toxicity to transgenic mosquitoes. We then define the line $\Gamma_{H^{**}}$ by

$$\Gamma_{H^{**}} \doteq \left\{(M,T)|M>0,\ T>0 \text{ and } M+\frac{1-m_1}{1-m_2}T = (1-m_1)H^*+\frac{1-m_1}{1-m_2}U\right\}.$$

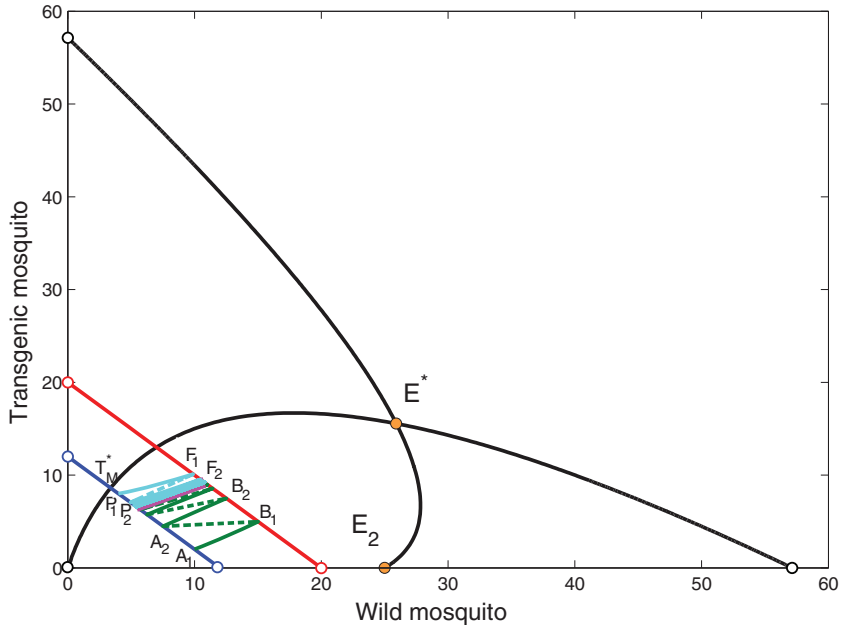

Fig. 10. The system (1) has a (purple) positive order-1 periodic solution. Here, $H^* = 20$, $H^{**} = 12$, $m_1 = m_2 = 0.5$, $a_1 = 0.4$, $a_2 = 0.7$, $b_1 = 0.7$, $b_2 = 0.2$, $\delta = 0.3$, $K = 100$ and $U = 2$. The red line represents the set Γ_{H^*}, the blue line represents the set $\Gamma_{H^{**}}$, the black curves represent the nullclines for wild and transgenic mosquitoes in the first quadrant and the purple curve represents a positive order-1 periodic solution. (For interpretation of the references to colour in this figure legend, the reader is referred to the web version of this article.)

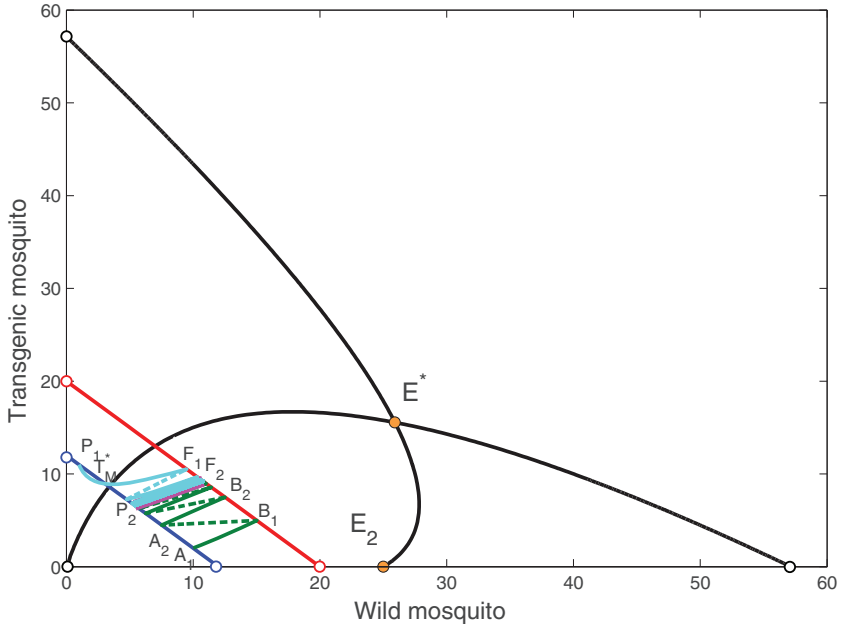

Fig. 11. The system (1) has a (purple) positive order-1 periodic solution. Here, $H^* = 20$, $H^{**} = 12$, $m_1 = m_2 = 0.5$, $a_1 = 0.4$, $a_2 = 0.7$, $b_1 = 0.7$, $b_2 = 0.2$, $\delta = 0.3$, $K = 100$ and $U = 2$. The red line represents the set Γ_{H^*}, the blue line represents the set $\Gamma_{H^{**}}$, the black curves represent the nullclines for wild and transgenic mosquitoes in the first quadrant and the purple curve represents a positive order-1 periodic solution. (For interpretation of the references to colour in this figure legend, the reader is referred to the web version of this article.)

Obviously, one notes that $U < m_2 H^*$ implies that the line: $M + T = H^*$ lies above the line: $M + \frac{1-m_1}{1-m_2} T = (1 - m_1)H^* + \frac{1-m_1}{1-m_2} U$ in the first quadrant. If this does not happen, then the second line might be unreachable.

In the following, we should consider three broad cases for the existence of positive periodic solutions. The proofs are similar to the one given above for the existence of positive periodic solutions in the case in which $m_1 = m_2$. On the other

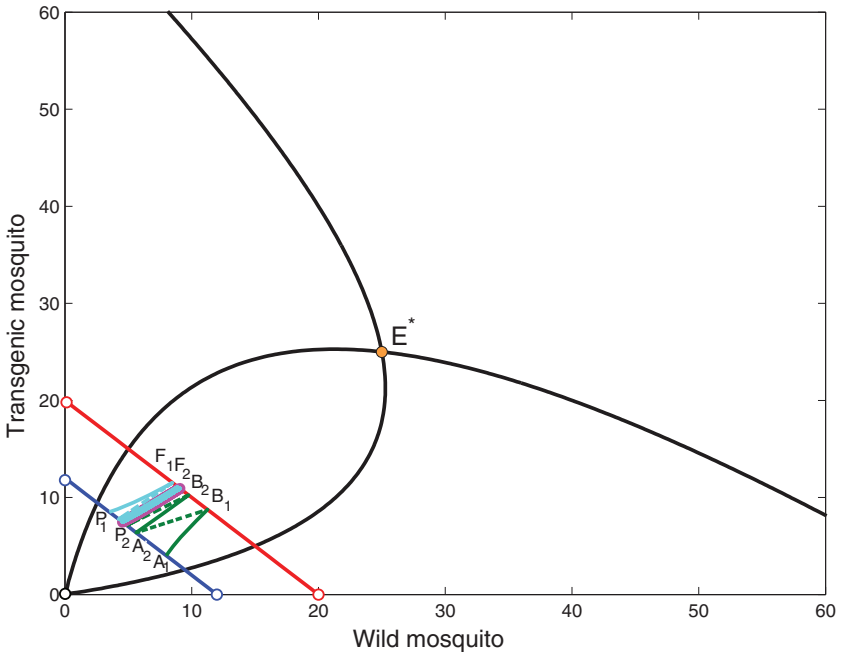

Fig. 12. The system (1) has a (purple) positive order-1 periodic solution. Here, $H^* = 20$, $H^{**} = 12$, $m_1 = m_2 = 0.5$, $a_1 = 0.1$, $a_2 = 0.7$, $b_1 = 0.7$, $b_2 = 0.1$, $\delta = 0.2$, $K = 100$ and $U = 2$. The red line represents the set Γ_{H^*}, the blue line represents the set $\Gamma_{H^{**}}$, the black curves represent the nullclines for wild and transgenic mosquitoes in the first quadrant and the purple curve represents a positive order-1 periodic solution. (For interpretation of the references to colour in this figure legend, the reader is referred to the web version of this article.)

hand, assuming that $m_1 < m_2$, one then notes that $U < \frac{(1-m_2)m_1}{1-m_1}H^*$ implies that the line $M + T = H^*$ lies above the line $T + \frac{1-m_2}{1-m_1}M = (1-m_2)H^* + U$ in the first quadrant. As a consequence, we obtain the following result.

Theorem 4.1. *For any $m_1, m_2 \in (0,1)$ such that $U < \min\{m_2, \frac{(1-m_2)m_1}{1-m_1}\}H^*$ and, in addition, if one of the following conditions holds:*

(i) *E_1 is stable with $K(b_1 - \delta) > b_1\big(\max\{1-m_1, 1-m_2\}H^* + U\big)$ and above the line Γ_{H^*} (that is, $H^* < \frac{K}{b_2}(b_2 - \delta)$);*
(ii) *E_2 is stable and above the line Γ_{H^*} for the system (2) (that is, $H^* < \frac{K}{a_1}(a_1 - \delta)$);*
(iii) *E^* is stable and above the line Γ_{H^*} for the system (2) (that is, $H^* < M^* + T^*$),*

then the system (1) admits a positive order-1 periodic solution.

4.2. Orbital asymptotic stability of positive order-1 periodic solutions

In this subsection, we shall consider the orbital asymptotic stability of positive order-1 periodic solutions of the system (1). To this purpose, let (μ^*, ν^*) be a positive order-1 periodic solution of the system (1) with period $\widetilde{T}$, which intersects the segments $\Gamma_{H^{**}}$ and Γ_{H^*} at the points $E^+\big((1-m_1)\mu^*(\widetilde{T}), (1-m_2)(H^* - \mu^*(\widetilde{T})) + U\big)$ and $E\big(\mu^*(\widetilde{T}), H^* - \mu^*(\widetilde{T})\big)$, respectively.

Theorem 4.2. *If*

$$\mu = \kappa \exp\left\{\int_0^{\widetilde{T}} \psi(t)dt\right\}$$

with

$$\kappa = \frac{A}{B}, \tag{22}$$

in which

$$\psi(t) = \frac{(a_1+a_2)(\mu^*(t))^2 + 2(a_1+b_2)\mu^*(t)\nu^*(t) + (b_1+b_2)(\nu^*(t))^2}{(\mu^*(t)+\nu^*(t))^2} - \frac{(2a_1+a_2)\mu^*(t) + (b_1+2b_2)\nu^*(t)}{K} - 2\delta,$$

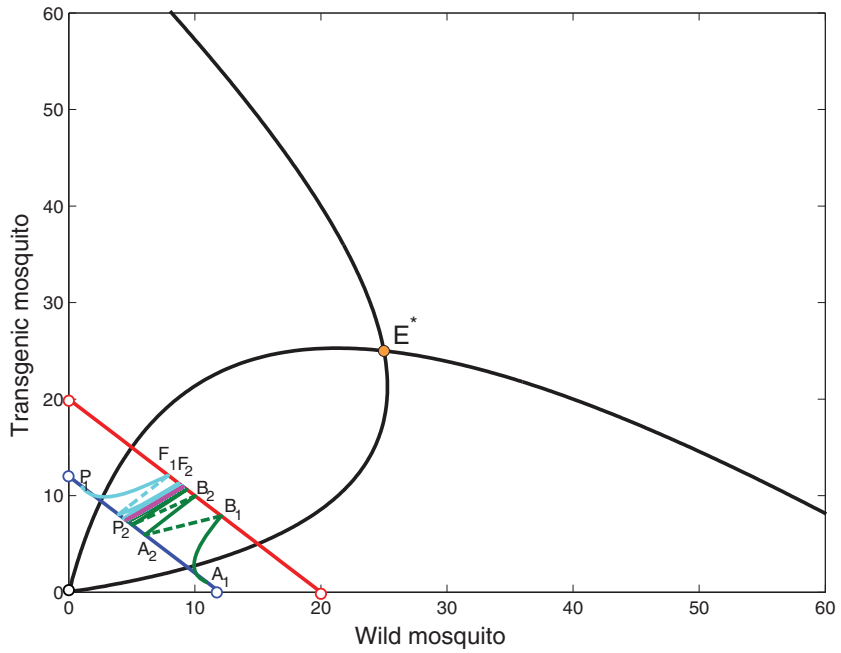

Fig. 13. The system (1) has a positive order-1 periodic solution (purple). Here $H^* = 20$, $H^{**} = 12$, $m_1 = m_2 = 0.5$, $a_1 = 0.1$, $a_2 = 0.7$, $b_1 = 0.7$, $b_2 = 0.1$, $\delta = 0.2$, $K = 100$ and $U = 2$. The red segment represents the set Γ_{H^*} and the blue segment represents the set $\Gamma_{H^{**}}$. (For interpretation of the references to colour in this figure legend, the reader is referred to the web version of this article.)

$$A = [(1-m_2)a_1(1-m_1)^2\mu^*(\widetilde{T})^2 + (1-m_1)b_2((1-m_2)(H^*-\mu^*(\widetilde{T}))+U)^2 + (a_2(1-m_1)+b_1(1-m_2))((1-m_1)\mu^*(\widetilde{T})((1-m_2)(H^*-\mu^*(\widetilde{T}))+U))] \cdot \left(\frac{1}{(m_2-m_1)\mu^*(\widetilde{T})+H^*(1-m_2)+U} - \frac{1}{K}\right) - \delta(1-m_1)((1-m_2)H^*+U)$$

and

$$B = (a_1(\mu^*(\widetilde{T}))^2 + b_2(H^*-\mu^*(\widetilde{T}))^2 + (a_2+b_1)\mu^*(\widetilde{T})(H^*-\mu^*(\widetilde{T})))\left(\frac{1}{H^*} - \frac{1}{K}\right) - \delta H^*,$$

then (μ^*, ν^*) *is orbitally asymptotically stable.*

Remark 4.3. If $m_1 = m_2$, then

$$\kappa = (1-m_1)\frac{A_1}{B_1},$$

in which

$$((\mu^*(\widetilde{T}^+), \nu^*(\widetilde{T}^+)) = ((1-m_1)\mu^*(\widetilde{T}), (1-m_1)H^* + U - (1-m_1)\mu^*(\widetilde{T}))$$

$$A_1 = (a_1(\mu^*(\widetilde{T}^+))^2 + b_2(\nu^*(\widetilde{T}^+))^2 + (a_2+b_1)\mu^*(\widetilde{T}^+)\nu^*(\widetilde{T}^+)) \cdot \frac{K-(1-m_1)H^*-U}{K((1-m_1)H^*+U)} - \delta((1-m_1)H^*+U)$$

$$B_1 = (a_1(\mu^*(\widetilde{T}))^2 + b_2(\nu^*(\widetilde{T}))^2 + (a_2+b_1)\mu^*(\widetilde{T})\nu^*(\widetilde{T}))\frac{K-H^*}{KH^*} - \delta H^*.$$

Without loss of generality, we here consider only the situation described in **Case** 1 of Table 1. Assume that $a_1 = 0.7$, $a_2 = 0.3$, $b_1 = 0.3$, $b_2 = 0.4$, $m_1 = 0.5$, $m_2 = 0.3$, $\delta = 0.1$, $K = 100$, $H^* = 60$ and $U = 1$. The graphs of the time series display periodic oscillations in the wild and transgenic mosquito populations with period $\widetilde{T} \approx 2.945,252,167,573$ (see Figs. 14 and 15). Also, according to the numerical simulations shown in Fig. 15, one notes that an approximate parametric equation of the positive order-1 periodic solution $(\widehat{\mu}^*, \widehat{\nu}^*)$ over a period is given by

$$\begin{cases} \widehat{\mu}^*(t) = 8.7751x - 4321.9, \\ \widehat{\nu}^*(t) = -0.10653x^2 + 106.43,089x^2 - 26,574, \end{cases} \qquad t \in [495.41, 548,058, 498.36,073,275). \tag{23}$$

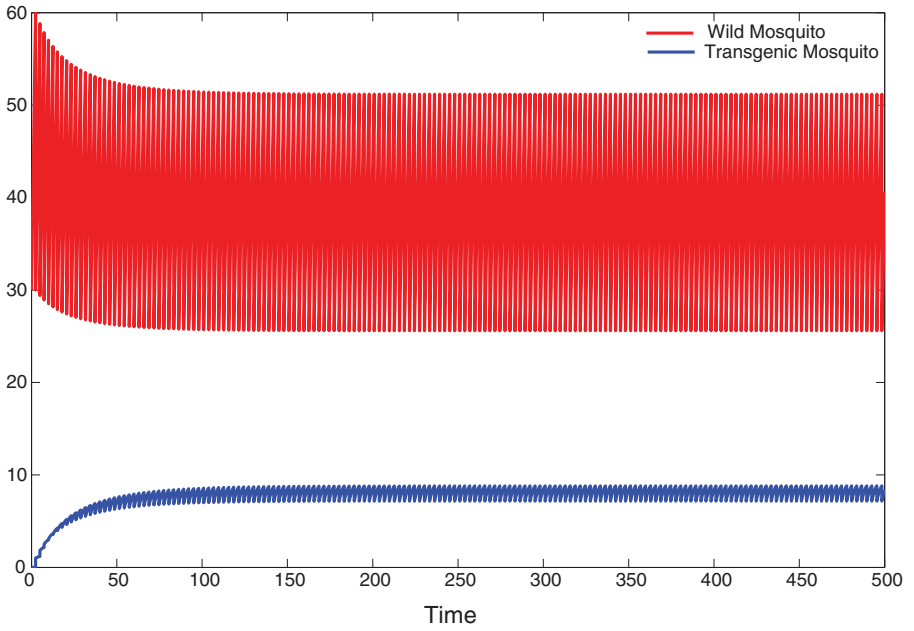

Fig. 14. Time series graphs of wild and transgenic mosquito populations. Here, $a_1 = 0.7$, $a_2 = 0.3$, $b_1 = 0.3$, $b_2 = 0.4$, $m_1 = 0.5$, $m_2 = 0.3$, $\delta = 0.1$, $K = 100$, $H^* = 60$ and $U = 1$. The initial conditions are $(M(0), T(0)) = (30, 0.01)$.

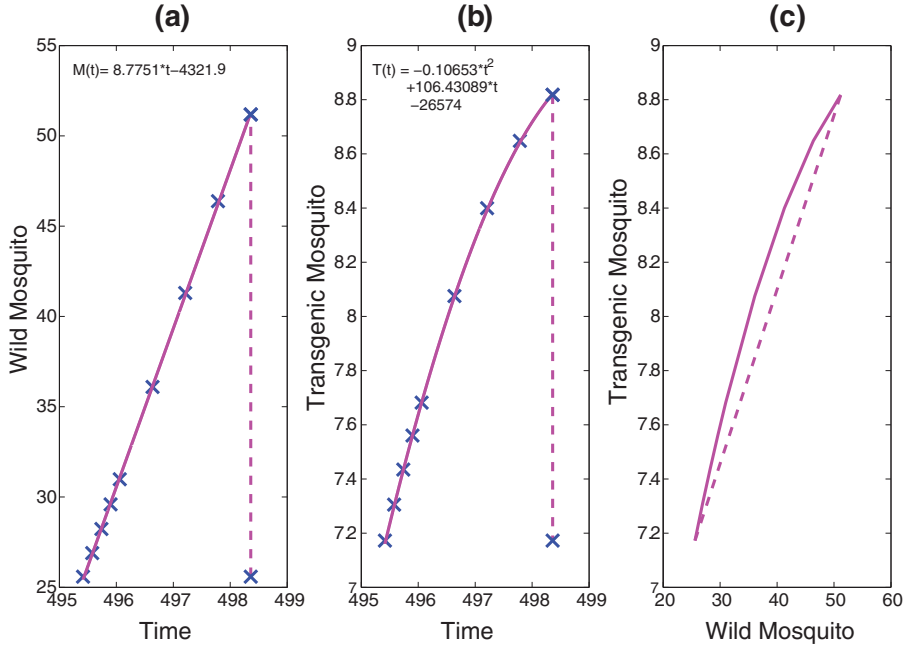

Fig. 15. (a) A time series graph of wild mosquito population over a period. (b) A time series graph of transgenic mosquito population over a period. (c) A phase diagram of positive order-1 periodic solution $(\widehat{\mu}^*, \widehat{\nu}^*)$. Here $a_1 = 0.7$, $a_2 = 0.3$, $b_1 = 0.3$, $b_2 = 0.4$, $m_1 = 0.5$, $m_2 = 0.3$, $\delta = 0.1$, $K = 100$, $H^* = 60$ and $U = 1$. The initial conditions are $(M(0), T(0)) = (30, 0.01)$. The period $\widetilde{T} \approx 2.945, 252, 167, 573$. Here, $t \in (495.415, 480, 583, 759, 498.360, 732, 751, 333]$.

At time $t = 498.36, 073, 275$, the periodic solution intersects the section Γ_{H^*} at the point $E(51.18, 8.82)$. The trajectory jumps then to the point $E^*(25.59, 7.174)$, due to the impulsive perturbations $M(t^+) = 0.5M(t)$ and $T(t^+) = 0.7T(t) + 1$, which occur when $M(t) + T(t) = 60$. Following the notations in Appendix B and the calculations in Appendix C, one obtains that

$$\kappa = 0.7286$$

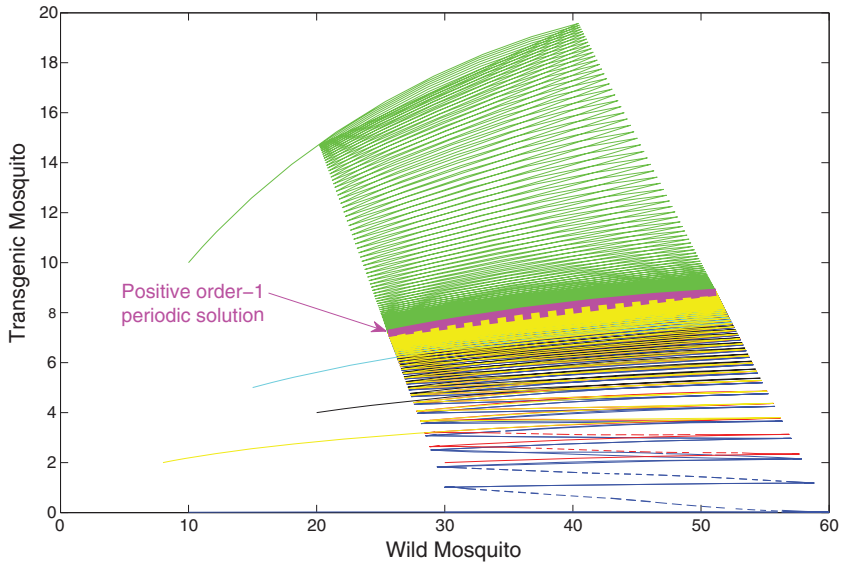

Fig. 16. The orbital asymptotic stability of the (magenta) positive order-1 periodic solution $(\widehat{\mu}^*, \widehat{v}^*)$. Here, $a_1 = 0.7$, $a_2 = 0.3$, $b_1 = 0.3$, $b_2 = 0.4$, $m_1 = 0.5$, $m_2 = 0.3$, $\delta = 0.1$, $K = 100$, $H^* = 60$ and $U = 1$. The blue curve represents the solution with initial conditions $(M(0), T(0)) = (10, 0.01)$. The red curve indicates the solution with initial conditions $(M(0), T(0)) = (30, 2)$. The black curve represents the solution with initial conditions $(M(0), T(0)) = (20, 4)$. The yellow curve indicates the solution with initial conditions $(M(0), T(0)) = (8, 2)$. The cyan curve indicates the solution with initial conditions $(M(0), T(0)) = (15, 5)$. The green curve represents the solution with initial conditions $(M(0), T(0)) = (10, 10)$. (For interpretation of the references to colour in this figure legend, the reader is referred to the web version of this article.)

and

$$\int_0^{\widetilde{T}} \left[\frac{\left(a_1 + a_2\right)(\widehat{\mu}^*(t))^2 + 2(a_1 + b_2)\widehat{\mu}^*(t)\widehat{v}^*(t) + \left(b_1 + b_2\right)(\widehat{v}^*(t))^2}{\left(\widehat{\mu}^*(t) + \widehat{v}^*(t)\right)^2} - \frac{\left(2a_1 + a_2\right)\widehat{\mu}^*(t) + \left(b_1 + 2b_2\right)\widehat{v}^*(t)}{K} - 2\delta \right] dt \approx -8.5e + 05.$$

which indicates that

$$\mu < 1.$$

Hence, the positive order-1 periodic solution $(\widehat{\mu}^*, \widehat{v}^*)$ is orbitally asymptotically stable as shown in Fig. 16.

5. Pareto efficient control of the wild mosquitoes

The pesticide-induced mortalities of wild and transgenic mosquitoes, expressed as percentages of the respective populations, are not actually constant, but rather variable, due to a variety of factors which include weather conditions such as wind direction and speed, temperature and relative humidity. However, for the sake of simplicity, we assume that the specified percentile mortalities induced by a pesticide dose u are

$$m_i = d_1^i\left(1 - \exp\left(-d_2^i u\right)\right), \ (i = 1, 2)$$

where $d_1^i \in (0, 1)$ is the maximal mortality rate and $d_2^i > 0$ is a dependence parameter.

Since it is usually impossible to eliminate the entire wild mosquito population, the next obvious choice is to keep its size as low as possible on a given interval $[T_0, \widehat{T}]$, while simultaneously keeping the control strategy near-optimal as far as the total cost is concerned. In this regard, it is useful to remember that wild and transgenic mosquitoes compete for the same blood meals and occupy the same habitat, which make the combined size of the mosquito populations restricted by the carrying capacity K.

In what follows, we recall the concept of Pareto efficiency in the context of the objectives

$$\underbrace{\int_{T_0}^{\widehat{T}} M(t)dt}_{\text{Total amount of the wild mosquito population}}$$

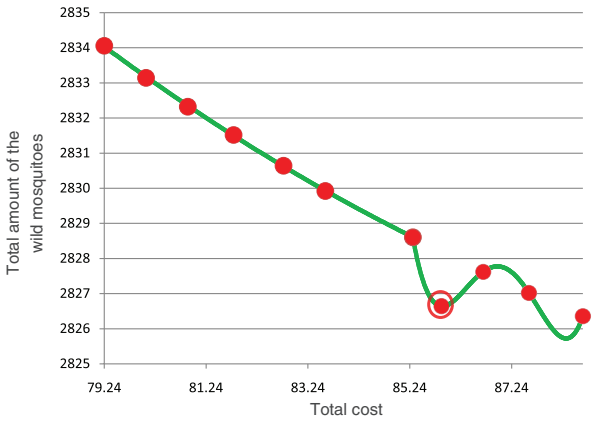

Fig. 17. The Pareto front with illustrative points marked. (For interpretation of the references to colour in the text, the reader is referred to the web version of this article.)

Table 2
Detailed information of the recommended impulsive control strategy.

No. of impulse	Time instance	Amount of pesticides	Amount of transgenic mosquitoes
i	τ_i	u_i	U_i
1	10.46	118	57
2	14.21	115	57
3	18.18	115	57
4	22.21	125	57
5	26.31	130	57

and

$$\underbrace{\sum_{i=1}^{N(\widehat{T})} (c_1 u_i + c_2 U_i)}_{\text{Total cost}}.$$

Here, u_i and U_i are the two control variables that represent the released amount of pesticides and, respectively, of transgenic mosquitoes when the phase point $(M(t), T(t))$ reaches the line Γ_{H^*} and $N(\widehat{T})$ is the number of the roots of the equation $M(t) + T(t) = H^*$, which equals the number of impulses. Also, c_1 is the unit price of pesticides and c_2 is the unit price of transgenic mosquitoes, which need to be raised in a lab. A control strategy is then said to be Pareto efficient if any change in the control strategy would make either the total cost higher or the total amount of the wild mosquitoes larger [31]. Here, we may always restrict our choices of control strategies to the Pareto front, which represents the set of all Pareto efficient strategies, without losing the best strategies due to this restriction.

In order to determine the Pareto frontier, we consider all admissible controls

$$\{(u, U)\} = \{(u_1, U_1), (u_2, U_2), \cdots, (u_{N(\widehat{T})}, U_{N(\widehat{T})})\}$$

that transfer the system (1) from a state $(M(T_0), T(T_0))$ into a state $(M(\widehat{T}), T(\widehat{T}))$ over a time interval $[T_0, \widehat{T}]$. Also, assume that τ_i, $i = 1, 2, \cdots, N(\widehat{T})$ are the instances at which the phase point $(M(t), T(t))$ reaches the line Γ_{H^*}. Note that $\widehat{T}$ is not fixed, but rather given by the condition that the phase point $(M(t), T(t))$ reaches the point $\big(M(\widehat{T}), T(\widehat{T})\big)$, $T_0 < \tau_1$ and $\tau_{N(\widehat{T})} < \widehat{T}$. We choose the following values of parameters: $a_1 = 0.1$, $a_2 = 0.8$, $b_1 = 0.8$, $b_2 = 0.1$, $K = 1000$, $\delta = 0.2$, $H^* = 300$, $d_1^1 = 0.6$, $d_2^1 = 0.03$, $d_1^2 = 0.7$, $d_2^2 = 0.015$, $c_0 = 1$, $c_1 = 0.08$, $c_2 = 0.66$, $T_0 = 0$, $\widehat{T} = 30$ and the initial conditions $\big(M(0), T(0)\big) = (50, 10)$. For the sake of simplicity, we set $(u, U) \in \{110, 111, \cdots, 130, \} \times \{50, 51, \cdots, 60\}$. Fig. 17 shows the Pareto frontier (green curve).

Consequently, the recommended strategy is the one described in Table 2, which leads to the dynamics of the wild mosquito population depicted in Fig. 18, with $N(30) = 5$ and the corresponding actuating effect given by $\{(u, U)\} = \{(118, 57), (115, 57), (115, 57), (125, 57), (130, 57)\}$. The trajectory of the wild mosquito population $M(t)$, $0 \le t \le 30$ shown in Fig. 18 appears to be a better objective than other different combinations since it remains near optimal in terms of the total size of the wild mosquito population over a time interval $[T_0, \widehat{T}]$ and is simultaneously not sensitive to the total cost.

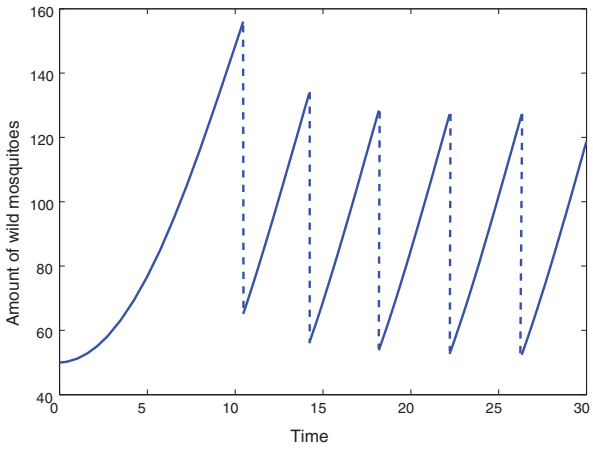

Fig. 18. The trajectory of the wild mosquito population corresponding to the recommended impulsive control strategy. Here $N(30) = 5$ and the actuating effect $\{(u, U)\} = \{(118, 57),\ (115, 57),\ (115, 57),\ (125, 57),\ (130, 57)\}$.

6. Concluding remarks

The present paper attempts to formulate and study a two-dimensional ODE model for the interaction between two wild and transgenic mosquito populations, which is subject to two control mechanisms employed simultaneously. It is assumed that the control measures occur in pulses and are triggered when the total density of the mosquito populations reaches a threshold value, which makes them impulsive and state-dependent.

To completely characterize the evolution of the system, we start by investigating its dynamics in the absence of perturbations. In this regard, we determine sufficient conditions for the existence and stability of the semi-trivial equilibria E_1 and E_2 in terms of the recruitment rates a_1, a_2, b_1, b_2 and of the death rate δ, finding in the process that the existence and stability of E_1 bear no relationship to the similar properties of E_2. Then, the existence and stability of the positive equilibria are characterized in terms of the same parameters. A certain exclusion property is observed to hold, in the sense that, if all three equilibria exist and the unique positive equilibrium is stable, then the semi-trivial equilibria are both unstable, and *vice versa*.

We then derive sufficient conditions for the existence and orbital stability of the positive order-1 periodic solutions, complementing our theoretical investigations by means of numerical simulations. It is observed that allowing the resetting set (the set which, when reached, triggers the control measures) to depend on several variables, as it is the case with our example, leads to a significantly richer dynamics of the system, compared to the situation in which the resetting set depends on a single variable [22,32].

To trade-off between multiple objectives, namely the total cost and the total size of the wild mosquito population, we employ the concept of Pareto efficiency to determine near-optimal controls. The Pareto frontier method presented here opens a new window for reconciling economic issues in pest management and can be easily extended to more complex scenarios. We expect the results obtained herein to be of use for minimizing the expenditure on the deployment of effective and sustainable pest control methods by concerned bodies, since the use of state-dependent controls leads to a reduction in the total mosquito size and to a more predictable growth pattern of the wild mosquito population.

The dynamics of a related predator–pest model subject to state-dependent feedback controls in which the resetting set depends upon a single variable, namely upon the density of the pest, has been discussed in [33], sufficient conditions for the existence and stability of semitrivial periodic solutions and of positive periodic solutions being established via a similar approach. Also, it has been shown in [33] that no positive order-q periodic solutions, $q \geq 3$, exist under a certain sufficient condition, amounting to the fact that the critical prey density at which the control measures are triggered is large enough. Further, it has been observed that if a certain threshold condition is reached, then a positive order-1 periodic solution emerges from the semitrivial periodic solution via a fold bifurcation. Potentially, the existence of positive order-q periodic solutions, $q \geq 2$, can be investigated for our model via a similar approach, although establishing ordering properties for the successive iterations of the Poincaré map of the control line or of the retreat line seems to be a difficult undertaking.

Another predator–pest model with logistic growth rates for both the pest and its predator and with Holling type I functional response for the predator has been considered in [34], the state-dependent controls being again employed when the size of the pest class reaches a certain critical value. The existence of order-1 and order-2 periodic solutions for a SIR epidemic model with state-dependent pulse vaccination has been discussed in [32], on condition that the vaccination occurs if the size of the infective class reaches a threshold value and, in the meantime, the size of the susceptible class is not less than the S-component of the positive equilibrium of the unperturbed system. Apart from considering a structurally different model and finding near-optimal

controls, we hereby consider a resetting set which is not parallel to a semi-axis, which echoes in a somewhat more complicated geometric analysis.

Acknowledgments

The work of H.Z. was supported by the National Natural Science Foundation of China, grant ID 11201187, the Scientific Research Foundation for the Returned Overseas Chinese Scholars and the China Scholarship Council. The work of P.G. was supported by a grant of the Romanian National Authority for Scientific Research, CNCS-UEFISCDI, project number PN-II-ID-PCE-2011-3-0563, contract no. 343/5.10.2011. L.Z. acknowledges the financial support from the Swedish Strategic Research Programme eSSENCE.

Appendix A. Orbital asymptotic stability

Let us define the distance between a point P and a set A in $\mathbf{R}^2$ by

$$d(P,A)=\inf\{d_E(P,Q);\,Q\in A\},$$

where by d_E we denote the usual Euclidean distance between points in $\mathbf{R}^2$. The trajectory $O^+\big(\big(M(t_0),T(t_0)\big),t_0\big)\big)$ starting at time t_0 in $(M(t_0),T(t_0))$ is said to be orbitally stable if for any given $\epsilon>0$, there exists a constant $\delta=\delta(\epsilon)>0$ such that for any other solution $\big(\widetilde{M},\widetilde{T}\big)$ of the system (1),

$$d((\widetilde{M}(t),\widetilde{T}(t)),O^+((M(t_0),T(t_0)),t_0)))<\epsilon$$

for all $t>t_0$ whenever

$$d((\widetilde{M}(t_0),\widetilde{T}(t_0)),O^+((M(t_0),T(t_0)),t_0)))<\delta.$$

The trajectory $O^+\big(\big(M(t_0),T(t_0)\big),t_0\big)\big)$ is said to be orbitally asymptotically stable if it is orbitally stable, and there exists a constant $\zeta>0$ such that for any other solution $(\widetilde{M},\widetilde{T})$ of the system (1),

$$d((\widetilde{M}(t),\widetilde{T}(t)),O^+((M(t_0),T(t_0)),t_0)))\to 0$$

as $t\to\infty$ whenever

$$d((\widetilde{M}(t_0),\widetilde{T}(t_0)),O^+((M(t_0),T(t_0)),t_0)))<\zeta.$$

Appendix B. Analogue of Poincaré criterion [17]

We consider the following autonomous system with state-dependent impulsive perturbations

$$\begin{cases}\frac{dx}{dt}=f(x,y), & \frac{dy}{dt}=g(x,y), & \text{if } \varphi(x,y)\neq 0,\\ \Delta x=\xi(x,y), & \Delta y=\eta(x,y), & \text{if } \varphi(x,y)=0,\end{cases}\tag{24}$$

in which f and g are continuous and differentiable functions defined on $\mathbf{R^2}$, φ is a sufficiently smooth function with $\nabla\varphi\neq 0$, and $\Delta x(t)=x(t+)-x(t)$, $\Delta y(t)=y(t+)-y(t)$.

Let (μ,ν) be a positive $\widetilde{T}$-periodic solution of the above system. The following result establishes a sufficient condition for its orbital asymptotic stability.

Lemma 6.1. *If the Floquet multiplier μ satisfies $|\mu|<1$, where*

$$\mu=\prod_{j=1}^{n}\kappa_j\exp\left\{\int_0^{\widetilde{T}}\left[\frac{\partial f(\mu(t),\nu(t))}{\partial x}+\frac{\partial g(\mu(t),\nu(t))}{\partial y}\right]dt\right\}$$

with

$$\kappa_j=\frac{\left(\frac{\partial\eta}{\partial y}\frac{\partial\varphi}{\partial x}-\frac{\partial\eta}{\partial x}\frac{\partial\varphi}{\partial y}+\frac{\partial\varphi}{\partial x}\right)f_+ +\left(\frac{\partial\xi}{\partial x}\frac{\partial\varphi}{\partial y}-\frac{\partial\xi}{\partial y}\frac{\partial\varphi}{\partial x}+\frac{\partial\varphi}{\partial y}\right)g_+}{\frac{\partial\varphi}{\partial x}f+\frac{\partial\varphi}{\partial y}g}$$

and $f,g,\frac{\partial\xi}{\partial x},\frac{\partial\xi}{\partial y},\frac{\partial\eta}{\partial x},\frac{\partial\eta}{\partial y},\frac{\partial\varphi}{\partial x}$, and $\frac{\partial\varphi}{\partial y}$ have been calculated at the point $(\mu(\tau_j),\nu(\tau_j))$, $f_+=f\big(\mu(\tau_j^+),\nu(\tau_j^+)\big)$, $g_+=g\big(\mu(\tau_j^+),\nu(\tau_j^+)\big)$, and $\tau_j(j\in\mathbf{N})$ is the time of the jth jump, $1\le j\le n$, n being the total number of impulsive perturbations in $[0,\widetilde{T}]$, then (μ,ν) is orbitally asymptotically stable.

Appendix C. Calculating κ and $\int_0^{\tilde{T}} \left[\frac{\partial f(\mu^*(t),\nu^*(t))}{\partial x} + \frac{\partial g(\mu^*(t),\nu^*(t))}{\partial y}\right]dt$

Following the notations in Appendix B, one determines that

$$\begin{aligned}
f(x,y) &= \left[\frac{a_1x+b_1y}{x+y}\left(1-\frac{x+y}{K}\right)-\delta\right]x,\\
g(x,y) &= \left[\frac{a_2x+b_2y}{x+y}\left(1-\frac{x+y}{K}\right)-\delta\right]y,\\
\xi(x,y) &= -m_1x,\\
\eta(x,y) &= -m_2y+U,\\
\varphi(x,y) &= x+y-H^*\\
(\mu^*(\tilde{T}),\nu^*(\tilde{T})) &= (\mu^*(\tilde{T}),H^*-\mu^*(\tilde{T})),\\
((\mu^*(\tilde{T}^+),\nu^*(\tilde{T}^+)) &= ((1-m_1)\mu^*(\tilde{T}),(1-m_2)(H^*-\mu^*(\tilde{T}))+U))
\end{aligned}$$

Consequently,

$$\begin{aligned}
&f(x,y)+g(x,y) = (a_1x^2+b_2y^2+(a_2+b_1)xy)\left(\frac{1}{x+y}-\frac{1}{K}\right)-\delta(x+y)\\
&(1-m_2)f(x,y)+(1-m_1)g(x,y) = ((1-m_2)a_1x^2+(1-m_1)b_2y^2+(a_2(1-m_1)+b_1(1-m_2))xy)\\
&\qquad\cdot\left(\frac{1}{x+y}-\frac{1}{K}\right)-\delta((1-m_2)x+(1-m_1)y)\\
&\frac{\partial f(x,y)}{\partial x} = \frac{a_1x^2+2b_1xy+b_1y^2}{(x+y)^2}-\frac{2a_1x+b_1y}{K}-\delta\\
&\frac{\partial g(x,y)}{\partial y} = \frac{a_2x^2+2b_2xy+b_2y^2}{(x+y)^2}-\frac{a_2x+2b_2y}{K}-\delta\\
&\frac{\partial\xi}{\partial x} = -m_1;\quad \frac{\partial\xi}{\partial y} = 0;\\
&\frac{\partial\eta}{\partial x} = 0;\quad \frac{\partial\eta}{\partial y} = -m_2\\
&\frac{\partial\varphi}{\partial x} = 1;\quad \frac{\partial\varphi}{\partial y} = 1.
\end{aligned}$$

It then follows that

$$\kappa = \frac{(1-m_2)f\left((\mu^*(\tilde{T}^+),\nu^*(\tilde{T}^+)\right)+(1-m_1)g\left((\mu^*(\tilde{T}^+),\nu^*(\tilde{T}^+)\right)}{f\left((\mu^*(\tilde{T}),\nu^*(\tilde{T})\right)+g\left((\mu^*(\tilde{T}),\nu^*(\tilde{T})\right)}$$

and

$$\int_0^{\tilde{T}}\left[\frac{\partial f(\mu^*(t),\nu^*(t))}{\partial x}+\frac{\partial g(\mu^*(t),\nu^*(t))}{\partial y}\right]dt = \int_{495.41548058}^{495.41548058+\tilde{T}}\left[\frac{\partial f(\mu^*(t),\nu^*(t))}{\partial x}+\frac{\partial g(\mu^*(t),\nu^*(t))}{\partial y}\right]dt.$$

References

[1] Gilles HM, Warrell DA, Bruce-Chwatt L. Bruce–Chwatt's essential malariology. London: Edward Arnold; 1993.
[2] Murray CJL, Rosenfeld LC, Lim SS, Andrews KG, Foreman KJ, Haring D, et al. Global malaria mortality between 1980 and 2010: a systematic analysis. Lancet 2011;379:413–31.
[3] Agnandji ST, Lell B, Soulanoudjingar SS, Fernandes JF, Abossolo BP, Conzelmann C, et al. A phase 3 trial of RTS, S/AS01 malaria vaccine in African infants. N Engl J Med 2012;367:2284–95.
[4] Muriu SM, Coulson T, Mbogo CM, Godfray H. Larval density dependence in *Anopheles gambiae* s.s., the major African vector of malaria. J Anim Ecol 2013;82:166–74.
[5] Brattsten LB, Hamilton G, Insecticides recommended for mosquito control in New Jersey in 2012. New Jersey Agricultural Experiment Station[publication no. P-08001-01-12].
[6] Weill M, Lutfalla G, Mogensen K, Chandre F, Berthomieu A, Berticat C, et al. Comparative genomics: insecticide resistance in mosquito vectors. Nature 2003;423:136–7.
[7] Ranson H, N'guessan R, Lines J, Moiroux N, Nkuni Z, Corbel V. Pyrethroid resistance in African anopheline mosquitoes: what are the implications for malaria control. Trends Parasitol 2011;27:91–8.
[8] Ito J, Ghosh A, Moreira LA, Wimmer EA, Jacobs-Lorena M. Transgenic anopheline mosquitoes impaired in transmission of a malaria parasite. Nature 2002;417:452–5.
[9] Catteruccia F, Nolan T, Loukeris TG, Blass C, Savakis C, Kafatos FC, Crisanti A. Stable germline transformation of the malaria mosquito *Anopheles stephensi*. Nature 2000;405:959–62.
[10] Brown AE, Bugeon L, Crisanti A, Catteruccia F. Stable and heritable gene silencing in the malaria vector *Anopheles stephensi*. Nucleic Acids Res 2003;31:e85.
[11] Bian G, Joshi D, Dong Y, Lu P, Zhou G, Pan X, et al. *Wolbachia* invades *Anopheles stephensi* populations and induces refractoriness to *Plasmodium* infection. Science 2013;340:748–51.

[12] Sperança MA, Capurro M. Perspectives in the control of infectious diseases by transgenic mosquitoes in the post-genomic era—a review. Mem Inst Oswaldo Cruz 2007;102:425–33.
[13] Kidwell MG, Ribeiro J. Can transposable elements be used to drive disease refractoriness genes into vector populations. Parasitol Today 1992;8:325–9.
[14] Boete C, Koella J. Evolutionary ideas about genetically manipulated mosquitoes and malaria control. Trends Parasitol 2003;19:32–8.
[15] Ross R. Studies on malaria. London: John Murray; 1928.
[16] Samoilenko AM, Perestyuk N. Impulsive differential equations. Singapore: World Scientific; 1995.
[17] Simeonov PS, Bainov D. Orbital stability of periodic solutions of autonomous systems with impulse effect. Int J Syst Sci 1988;19:2561–85.
[18] Jiang GR, Lu Q. The dynamics of a prey–predator model with impulsive state feedback control. Discrete Contin Dyn Syst Ser B 2006;6:1310–20.
[19] Jiang GR, Lu Q. Impulsive state feedback control of a predator–prey model. J Comput Appl Math 2007;200:193–207.
[20] Jiao J, Chen L, Long W. Pulse fishing policy for a stage-structured model with state-dependent harvesting. J Biol Syst 2007;15:409–16.
[21] Tang SY, Xiao YN, Chen LS, Cheke R. Integrated pest management models and their dynamical behaviour. Bull Math Biol 2005;67:115–35.
[22] Nie LF, Teng ZD, Guo B. A state dependent pulse control strategy for a SIRS epidemic system. Bull Math Biol 2013;75:1697–715.
[23] Guo HJ, Chen L. Periodic solution of a chemostat model with Monod growth rate and impulsive state feedback control. J Theor Biol 2009;260:502–9.
[24] Tian Y, Sun KB, Chen LS, Kasperski A. Studies on the dynamics of a continuous bioprocess with impulsive state feedback control. Chem Eng J 2010;157:558–67.
[25] Li J. Simple mathematical models for interacting wild and transgenic mosquito population. Math Biosci 2004;189:39–59.
[26] Rafikov M, Bevilacqua L, Wyse AP. Optimal control strategy of malaria vector using genetically modified mosquitoes. J Theor Biol 2009;258:418–25.
[27] Damalas CA, Eleftherohorinos I. Pesticide exposure, safety issues, and risk assessment indicators. Int J Environ Res Public Health 2011;8:1402–19.
[28] Georgescu P, Hsieh Y. Global dynamics of a predator–prey model with stage structure for the predator. SIAM J Appl Math 2007;67:1379–95.
[29] Terry A. Prey resurgence from mortality events in predator–prey models. Nonlinear Anal: Real World Appl 2013;14:2180–21203.
[30] Sastry S. Nonlinear systems: analysis, stability, and control. New York: Springer-Verlag; 1999.
[31] Mathur V. How well do we know Pareto optimality. J Econ Educ 1991;22:172–8.
[32] Nie L, Teng Z, Torres A. Dynamic analysis of a SIR epidemic model with state-dependent pulse vaccination. Nonlinear Anal: Real World Appl 2012;13:1621–9.
[33] Baek H. The dynamics of a predator–prey system with state-dependent feedback control. Abstract Appl Anal 2012.
[34] Xiao Q, Dai B. Dynamics of an impulsive predator–prey logistic population model with state-dependent. Appl Math Comput 2015;259:220–30.